University of Glasgow

Maddocks, O. D.K. et al. (2017) Modulating the therapeutic response of tumours to dietary serine and glycine starvation. Nature, 544(7650), pp. 372-376.

There may be differences between this version and the published version. You are advised to consult the publisher's version if you wish to cite from it.

http://eprints.gla.ac.uk/140432/

Deposited on: 25 May 2017

Modulating the therapeutic response of tumours to dietary serine and glycine starvation

Oliver D. K. Maddocks[1,2], Dimitris Athineos[1], Eric C. Cheung[1], Pearl Lee[1†], Tong Zhang[2], Niels J. F. van den Broek[1], Gillian M. Mackay[1], Christiaan F. Labuschagne[1], David Gay[1], Flore Kruiswijk[1], Julianna Blagih[1], David F. Vincent[1], Kirsteen J. Campbell[1], Fatih Ceteci[1†], Owen J. Sansom[1], Karen Blyth[1] & Karen H. Vousden[1†].

[1] Cancer Research UK Beatson Institute, Switchback Road, Glasgow G61 1BD, UK

[2] University of Glasgow Institute of Cancer Sciences, Switchback Road, Glasgow G61 1QH, UK

[†] Present addresses: Abrahamson Family Cancer Research Institute, 421 Curie Boulevard, Philadelphia, Pennsylvania 19104, USA (P.L.); Institute for Tumor Biology and Experimental Therapy, Georg-Speyer-Haus, Paul-Ehrlich-Strasse 42-44, 60596 Frankfurt am Main, Germany (F.C.); The Crick Institute, 1 Midland Road, London NW1 1AT, UK (K.H.V.).

Abstract

The non-essential amino acids serine and glycine are used in multiple anabolic processes that support cancer cell growth and proliferation (reviewed in ref. 1). While some cancer cells upregulate de novo serine synthesis[2, 3, 4], many others rely on exogenous serine for optimal growth[5, 6, 7]. Restriction of dietary serine and glycine can reduce tumour growth in xenograft and allograft models[7, 8]. Here we show that this observation translates into more clinically relevant autochthonous tumours in genetically engineered mouse models of intestinal cancer (driven by Apc inactivation) or lymphoma (driven by Myc activation). The increased survival following dietary restriction of serine and glycine in these models was further improved by antagonizing the anti-oxidant response. Disruption of mitochondrial oxidative phosphorylation (using biguanides) led to a complex response that could improve or impede the anti-tumour effect of serine and glycine starvation. Notably, Kras-driven mouse models of pancreatic and intestinal cancers were less responsive to depletion of serine and glycine, reflecting an ability of activated Kras to increase the expression of enzymes that are part of the serine synthesis pathway and thus promote de novo serine synthesis.

To assess the effect of dietary serine and glycine (SG) restriction in autochthonous tumour models, we used genetically engineered mouse models (GEMMs) of lymphoma (*Eμ-Myc*) and intestinal tumours (defective *Apc*). *Eμ-Myc* mice develop pre-neoplastic lesions within 28–42 days after birth[9], and adenoma initiation is evident days after birth in *Apc*[Min/+] mice[10]. Accordingly, *Apc*[Min/+]mice carried high tumour numbers at 80 days, which subsequently increased in size but not number (Extended Data Fig. 1a). Transferring mice from normal chow diet to experimental diets 60–80 days after birth showed that an SG-free diet significantly extended survival in these models carrying pre-malignant lesions (Fig. 1a, b), with a slightly lower tumour burden in *Apc*[Min/+] mice on the SG-free diet at clinical end point (Extended Data Fig. 1a). The diet reproducibly decreased serum SG from around 150 μM to 65 μM (Fig. 1c–e), while showing minimal or inconsistent impact on other amino acids, glucose and lactate (Fig. 1c, d and Extended Data Figs 1b, 2a, b), These results were further validated using an inducible intestinal tumour model (*Lgr5-creER;Apc*^{fl/fl}); transferring mice to the SG-free diet a week after induction. Again, the experimental diet caused a significant increase in survival compared to control diet (containing purified amino acids) or normal chow (containing whole protein as a source of amino acids) (Fig. 1f).

Figure 1: SG-free diet is an effective therapeutic intervention in GEMMs for lymphoma and intestinal cancer.
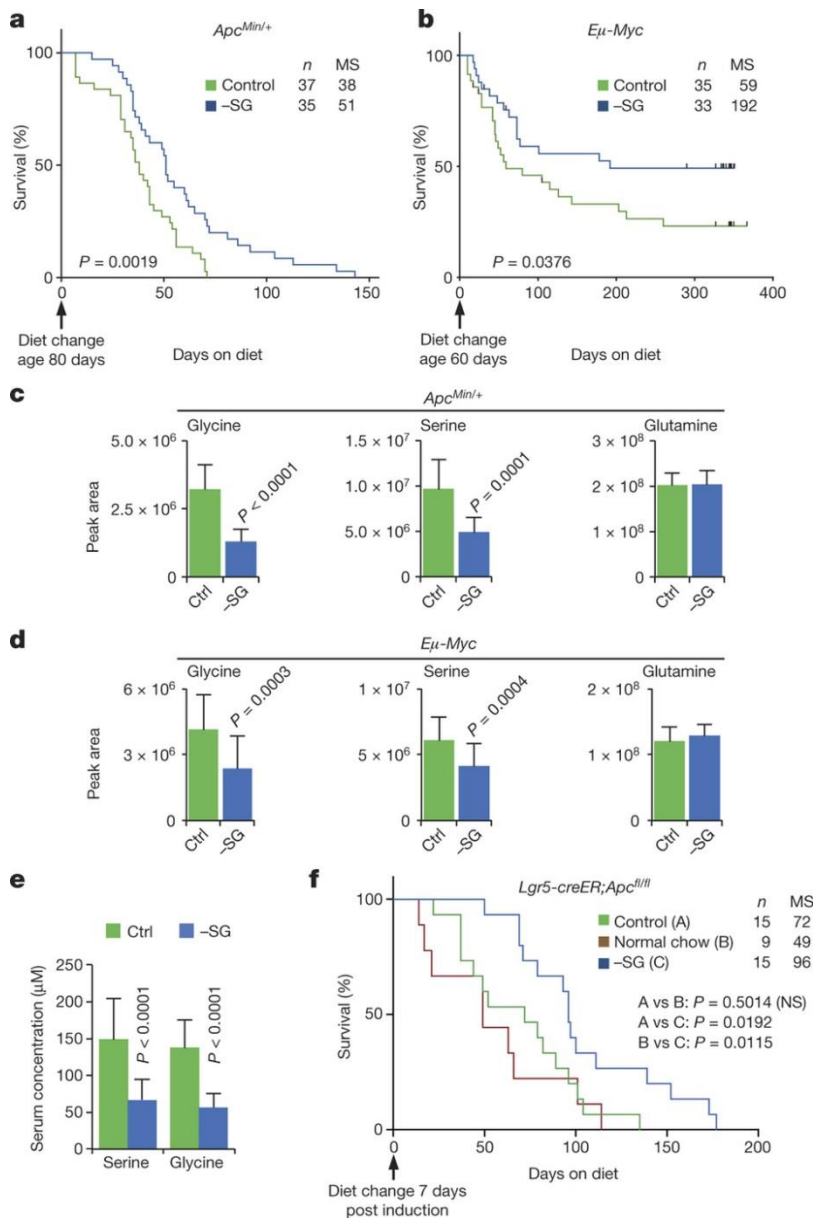
a, *Apc^Min/+* mice received normal chow until 80 days of age, then were transferred to either a control diet (containing SG) or a matched diet lacking SG (−SG) until clinical end point (intestinal-tumour-related survival). Survival was calculated from change of diet. See Source Data. **b**, *Eμ-Myc* mice received normal chow until 60 days of age, then were transferred to either a control diet (containing SG) or a matched diet lacking SG until clinical end point (lymphoma-related survival). Survival was calculated from change of diet. See Source Data. **c**, **d**, Serum samples from *Apc^Min/+* (**c**, control, $n = 14$; −SG, $n = 13$) and *Eμ-Myc* (**d**, control, $n = 24$; −SG, $n = 24$) cohorts were analysed by liquid chromatography–mass spectrometry (LC–MS), relative abundance (by metabolite peak area) is shown. Ctrl, control. Error bars are s.d., *P* values were calculated by *t*-test (unpaired, two-tailed). See Extended Data Fig. 2 for relative quantification of all amino acids. **e**, Serum concentration for serine and glycine in the *Apc^Min/+* cohort (control, $n = 14$; −SG, $n = 13$) was determined using six-point calibration curves with ^{13}C–^{15}N-labelled serine and glycine diluted in serum. Error bars are s.d., *P* values were calculated by *t*-test (unpaired, two-tailed). **f**, *Lgr5-creER;Apc^fl/fl* mice were induced at 7–10 weeks of age, diet was changed seven days after first tamoxifen treatment and maintained until clinical end point (intestinal-tumour-related survival). Survival is calculated from first tamoxifen treatment. For all survival plots, *P* values calculated by Mantel–Cox test; NS, not significant. *n*, number of mice; MS, median survival in days. See Source Data.

To test the effect of SG starvation on larger, established tumours (to mimic a therapeutic intervention), we transferred mice carrying measurable HCT116 (an invasive human colorectal cancer cell line) tumours onto the SG-free diet, which significantly retarded tumour growth (Extended Data Fig. 3a). The *in vitro* growth of HCT116 cells was similarly diminished (in a cell-autonomous context) under SG concentrations detected in tumours (Extended Data Fig. 3b–d). Using subcutaneous allografts of *Eµ-Myc* tumour cells, we transferred mice to SG-free diet after tumour formation and collected the tumours at a single temporal end point (6 days post diet change). Even with this relatively short period of SG restriction, a trend towards decreased tumour volume and cell number was seen, although no differences in cleaved caspase-3 (a marker of apoptosis) or BrdU incorporation (a marker of proliferation) were detected (Extended Data Fig. 4a–c). However, haematoxylin and eosin staining showed a clear increase in necrosis in cross-sections of tumours from mice on the SG-free diet (Extended Data Fig. 4d, e). *Apc*$^{Min/+}$ mice analysed at temporal end point (14 days post diet change) showed a trend for decreased cell number and increased apoptosis (Extended Data Fig. 4f) but no evidence of necrosis, suggesting that tumour-specific factors, such as tissue of origin, tumour size and proliferation rate, influence tumour response.

Serine starvation activates *de novo* serine synthesis, diverting glycolytic intermediates away from energy production[11, 12]. Cells respond by increasing oxidative phosphorylation to maintain ATP turnover, and inhibiting oxidative phosphorylation (for example, by using biguanides to inhibit mitochondrial complex I) can enhance the anti-proliferative effect of serine starvation[7, 8]. A maximal dose (100 mg kg^{-1} per day)[13] of the biguanide phenformin was tolerated by *Eµ-Myc* mice on the control diet, but elicited marked toxicity (symptoms resembling dyschezia) in *Eµ-Myc* mice on the SG-free diet. While this prevented further recruitment, mice that survived on the SG-free diet with phenformin (7/14) did not suffer further adverse effects, and showed a trend for improved survival compared to animals on the SG-free diet alone (Fig. 2a), consistent with a previous study in a tumour allograft system[8].

Figure 2: Manipulation of anti-oxidant response enhanced diet-induced anti-cancer effect.
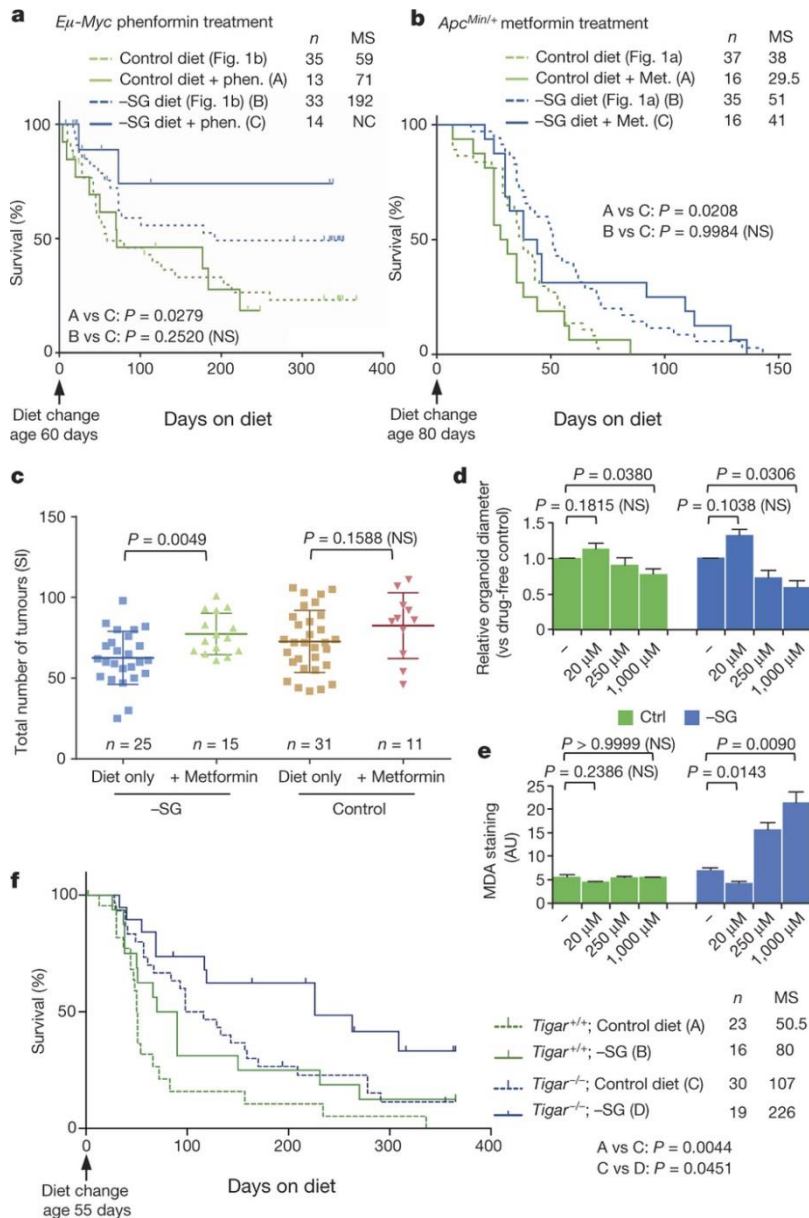
a, *Eμ-Myc* mice received control or SG-free diet (−SG) with 100 mg kg⁻¹ per day phenformin by gavage at 60 days of age and taken to clinical end point. Lymphoma-related survival was calculated from change of diet. Mice in the SG-free diet plus phenformin cohort that were removed due to phenformin-related toxicity are included as censored observations in the survival plot. See Source Data. **b**, *Apc^{Min/+}* mice were transferred to control or SG-free diet at 80 days of age, then five days later received metformin 200 mg kg⁻¹ per day in drinking water. Intestinal-tumour-related survival calculated from change of diet. See Extended Data Fig. 5a for complete comparison of survival curves. See Source Data. For ease of comparison, dashed lines indicating survival from diet-only cohorts shown in Fig. 1a, b are replicated in **a**, **b**. **c**, Post-mortem count of tumour number was performed on the small intestine (SI) of *Apc^{Min/+}* mice. *P* values calculated by *t*-test (unpaired, two-tailed). Diet-only tumour number also shown in Extended Data Fig. 1a. See Extended Data Fig. 5b for tumour area data. See Source Data. **d**, Intestinal tumour organoids derived from a *Vil1-creER;Apc^{fl/fl}* mouse were grown with or without SG and with or without metformin at the stated concentrations for two days. Relative change (versus drug-free control) in organoid diameter is plotted. Data are average of four independent experiments, error bars are s.e.m. *P* values calculated by *t*-test (unpaired, two-tailed, corrected for multiple comparisons). **e**, *Vil1-creER;Apc^{fl/fl}* organoids were grown with or without SG and with or without metformin for two days, then fixed and immunostained for lipid peroxidation product malondialdehyde (MDA). Data are average of three independent experiments, error bars are s.e.m. *P* values calculated by *t*-test (unpaired, two-tailed, corrected for multiple comparisons). **f**, *Eμ-Myc* mice were crossed with *Tigar^{−/−}* mice, cohorts were placed on diets at 55 days of age and taken

Metformin is a biguanide with lower toxicity than phenformin that is widely used in the clinic as an anti-diabetic agent and is being trialled as an anti-cancer agent[14]. While systemic availability of oral metformin is generally poor, some tissues (including the intestine) express OCT1 transporters that facilitate metformin uptake[15]. In humans, metformin doses of 0.5–1 g per day have been used in multiple clinical trials in colorectal cancer[14]. Using a dose of metformin (200 mg kg^{-1} per day) in mice equivalent (by body surface area calculation[16]) to a daily human dose of 1 g per day, we failed to detect a significant impact of metformin on the survival of *Apc^Min/+* mice, although the beneficial effect of SG-starvation persisted (Fig. 2b and Extended Data Fig. 5a). Intriguingly, metformin increased the number of tumours in the SG-free diet group (Fig. 2c), without impacting average tumour area (Extended Data Fig. 5b).

Serum metformin ranged from 2 to 22 µM in *Apc^Min/+* mice, with tissue metformin concentration ranging from 0.1 to 11 µM (Extended Data Fig. 6a–c), consistent with metformin pharmacokinetics in other tumour-bearing mice given metformin in drinking water[17, 18]. No difference in serum glucose and lactate levels were seen (Extended Data Fig. 6d), indicating that this dose had minimal impact on systemic metabolism. Using *Vil1-creER;Apc^fl/fl* mouse-derived organoids to assess the cell-autonomous effects of metformin showed that high metformin doses inhibited organoid growth as expected. Notably, a lower metformin dose (20 µM) tended to increase organoid size (Fig. 2d), although this did not reach statistical significance. While complex I inhibition by biguanides can increase the levels of reactive oxygen species (ROS), metformin also has anti-oxidant properties[19,20, 21, 22] and we have shown that limiting ROS improves cell survival during SG starvation[7]. Consistently, under SG starvation, low-dose metformin decreased ROS levels, while higher doses increased ROS (Fig. 2e). Treatment of SG-starved organoids with another ROS inducer (daunorubicin) decreased growth and increased ROS at low and high doses (Extended Data Fig. 6e, f). The differential effect of metformin on the response to SG starvation therefore correlates with its potential anti- and pro-oxidant effects, although further studies will be necessary to fully explore the role of biguanides and ROS in this context.

Our study suggests that the metformin levels achieved in our GEMMs were too low to inhibit tumour growth. Although the metformin doses used here were comparable with clinically effective doses for diabetes treatment in humans, species differences in the pharmacodynamics and/or pharmacokinetics of metformin could make it difficult to translate these responses from mouse to humans[17, 18]. While the response to metformin is dose-dependent, our data support the results of *in vitro* studies that show that manipulating ROS can modulate the response of tumours to SG starvation[7]. To test directly whether increasing ROS *in vivo* could enhance the anti-tumour effect of the SG-free diet, we used *Tigar^-/-* mice that do not express Tigar, a protein that can support tumour development by limiting ROS[23, 24, 25, 26]. While *Eµ-Myc* expression on this mixed strain background caused mice to die of lymphoma more rapidly than pure BL6 *Eµ-Myc* mice (shown in Fig. 2a), a combination of *Tigar* deletion with SG-free diet produced a significantly additive overall increase in survival (Fig. 2f). Many chemotherapeutics and radiotherapy induce ROS, suggesting that there may be a benefit to combining this diet with standard anti-cancer treatments.

Previous studies have shown that the response to SG starvation can be modulated by other genetic alterations in the tumour, including amplification of the serine synthesis pathway (SSP) enzymes (making cells less reliant on extracellular serine) or loss of the tumour suppressor p53 (increasing

vulnerability to serine starvation)[3,7]. Surprisingly, two mouse models of pancreatic cancer (PDAC) driven by activation of Kras with either loss (*Pdx1-cre;Kras[G12D/+];Trp53^{fl/+}*) or mutation (*Pdx1-cre;Kras[G12D/+];Trp53[R172H/+]*) of p53[27,28] showed no significant change in survival in response to SG-free diet, despite a clear decrease in serum SG levels (Fig. 3a and Extended Data Figs 7, 8a, b). Intravenous injection of ^{13}C–^{15}N-labelled serine revealed that serine uptake was comparable in normal pancreatic and tumour tissue, whereas intestinal tumours in the *Apc[Min/+]* model took up significantly more serine (with subsequent conversion to glycine) compared to normal intestinal tissue (Fig. 3b). In contrast to the *Apc[Min/+]* tumours, *Kras* mutant pancreatic tumours appeared to be less reliant on exogenous serine, explaining their resistance to the diet.

*Figure 3: Activated Kras confers resistance to the anti-cancer effects of SG-free diet.*
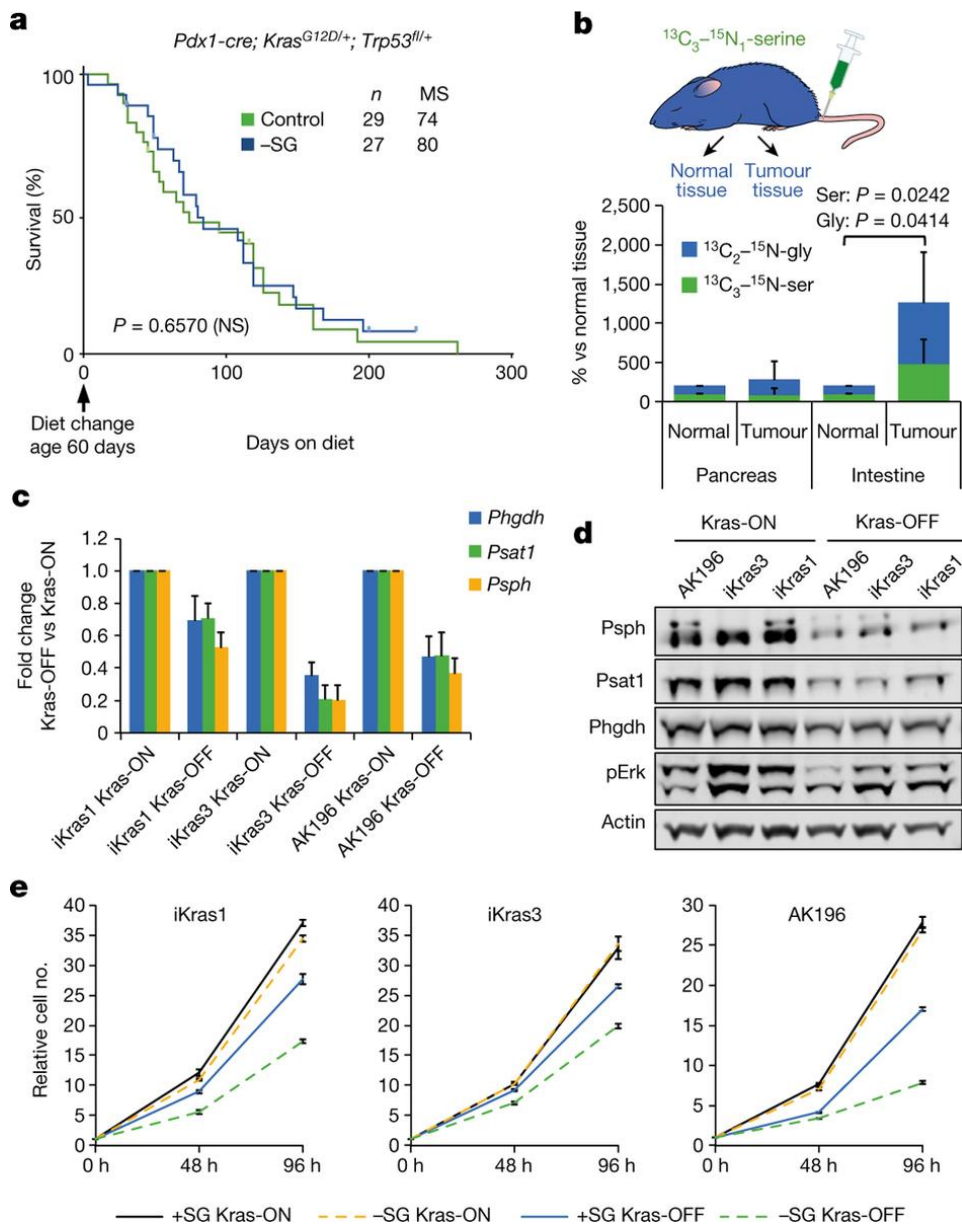
a, *Pdx1-cre;Kras[G12D/+];Trp53^{fl/+}* mice received control or SG-free (−SG) diet at 60 days of age until clinical end point. PDAC-related survival was calculated from change of diet. *P* value calculated by Mantel–Cox test. *n*, number of mice; MS, median survival in days. See Source Data. **b**, *Pdx1-cre;Kras[G12D/+];Trp53[R172H/+]* mice (*n* = 3), non-cre-expressing isogenic control mice with normal pancreas (*n* = 3) and *Apc[Min/+]* mice (*n* = 3) were injected in the tail vein with 100 µl of 100 mM ^{13}C$_3$–^{15}N$_1$-serine

and left for 2 h. PDAC/normal pancreas/intestinal adenoma/normal intestine tissue were excised and analysed by LC–MS. *P* values were calculated using *t*-test (unpaired for pancreas, paired for intestine, one-tailed). Error bars are s.d. **c**, Kras-inducible cell lines (iKras1, iKras3 and AK196) were grown in complete medium with doxycycline (Kras-ON) or without doxycycline (Kras-OFF) for 48 h. Messenger RNA expression of serine synthesis pathway enzymes was analysed by qRT–PCR. Data are average of three independent experiments each performed with technical duplicates, error bars are s.e.m. **d**, Kras-inducible cell lines were grown with or without doxycycline for 72 h, protein expression was analysed by western blot. For gel source data, see Supplementary Fig. 1. See Extended Data Fig. 10a for quantification of changes in expression. **e**, Kras-inducible cell lines were grown in medium with or without serine and glycine and counted after 48 and 96 h. Data are averages of three independent experiments, each performed in triplicate for each condition, error bars are s.e.m.

Kras can reprogram glucose and glutamine metabolism to support anabolism and redox balance[29,30], but the SG-free diet did not significantly alter serum glutamine, glucose or lactate (Extended Data Figs 7, 8b, c), or Ampk phosphorylation in PDAC (or *Eμ-Myc*) tumours (Extended Data Fig. 9a). Activated Kras increases protein scavenging by macropinocytosis, a mechanism likely to make cells less dependent on circulating serine levels[31,32]. However, we did not detect any change in macropinocytosis in pancreatic cells with doxycycline-inducible *Kras^G12D*(ref. 30) in response to SG starvation (Extended Data Fig. 9b). Activated Kras also increases the transcription of *Nrf2* (ref. 33), which can drive SSP enzyme expression[34], potentially negating dependence on extracellular serine. Using the *Kras^G12D*-inducible cells, we found a consistent decrease in SSP enzyme expression at both the RNA and protein level following downregulation of Kras expression (Fig. 3c, d and Extended Data Fig. 9c). Cells induced to express activated Kras were resistant to SG starvation, whereas non-induced cells were sensitive to SG starvation (Fig. 3e). PDAC tumours of both genotypes responded to dietary SG restriction by upregulating SSP enzyme expression, a response that was not seen in the starvation-sensitive *Eμ-Myc* tumours (which do not have activated Kras) (Extended Data Fig. 9d). Glycine levels and the GSH/GSSG ratio were maintained in PDAC but not *Eμ-Myc* tumours on SG-free diet (Extended Data Fig. 10a). Unbiased metabolomics confirmed that serine and glycine were the major metabolites depleted by the diet in tumours from *Eμ-Myc* mice (Extended Data Fig. 10b).

Vil1-creER;Apc^{fl/fl} intestinal tumour organoids grow rapidly *in vitro*, but after five days in SG-free medium their ability to recover and grow was severely impaired. Addition of activated Kras allowed recovery from starvation and continued growth (Fig. 4a, b). These differences were reflected in higher basal expression of the genes encoding SSP enzymes in the activated Kras-expressing cells (Fig. 4c). Growth of organoids in labelled glucose showed that labelled serine levels (derived from glucose through the SSP) were higher in the *Kras^G12D* cells, indicating increased rates of serine synthesis (Fig. 4d). Analysis of *Vil1-creER;Apc^{fl/fl}* and *Vil1-creER;Apc^{fl/fl};Kras^{G12D/+}*intestinal tissue showed that while Apc deregulation alone increased *Psat1* and *Psph* expression—probably reflecting the ability of β-catenin-driven Myc to support SSP expression[34]—the addition of activated Kras further enhanced SSP enzyme expression (Fig. 4e). Finally, we wished to assess the effect of Kras activation in an intestinal GEMM. *Vil1-creER;Apc^{fl/fl};Kras^{G12D/+}* mice die within five days of induction due to hyperproliferative crypts, while addition of *Kras^G12D* to the *Lgr5-creER;Apc^{fl/fl}* model markedly accelerates tumour development. Therefore, to allow comparison with the Apc-only models employed so far, we used *Vil1-creER;Apc^{fl/+};Kras^{G12D/+}* mice, which have survival times comparable to our Apc-only models, and transferred mice to diet before Cre induction. In line with the ability of activated Kras to upregulate SSP enzyme expression, *Kras^G12D* expression abrogated the pro-survival effect of the SG-free diet (Fig. 4f), although a trend for decreased tumour area was retained (Extended Data Fig. 10c).

Figure 4: Kras(G12D)-expressing cells resist SG starvation by upregulating de novo serine synthesis.
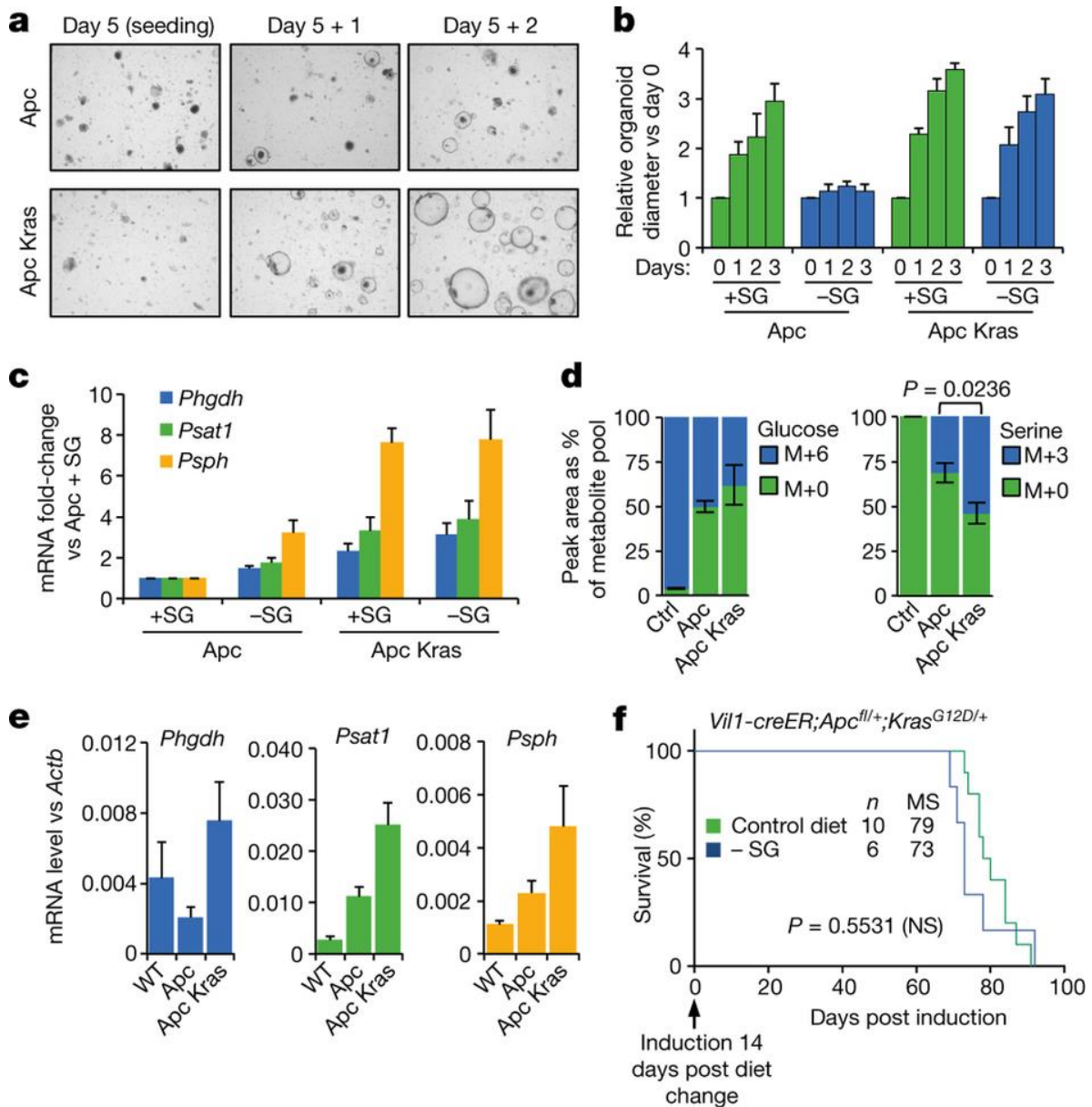
a, *Vil1-creER;Apc^{fl/fl}* (Apc) and *Vil1-creER;Apc^{fl/fl};Kras^{G12D/+}* (Apc Kras) intestinal tumour organoids (from n = 3 mice per genotype) were grown without SG for five days then dissociated and seeded into complete growth medium. Representative images of the organoids are shown on day 5 (after seeding), and after 1 and 2 days of recovery. **b**, Organoid diameter was measured for each day in complete (recovery) medium. Data are averages of organoids from three mice, obtained in a single experiment, error bars are s.e.m. **c**, Messenger RNA was extracted from *Vil1-creER;Apc^{fl/fl}* and *Vil1-creER;Apc^{fl/fl};Kras^{G12D/+}* organoids grown with or without SG for 48 h and analysis of SSP enzyme expression was performed using qRT–PCR (n = 3 mice per genotype, qRT–PCR performed in technical triplicate). Error bars are s.e.m. **d**, Organoids (from n = 3 mice per genotype) were grown in the presence of $^{13}C_6$-glucose for 5 h, metabolites were extracted and analysed by LC–MS. Wells containing Matrigel only were used as controls. Error bars are s.d. P values calculated by t-test (unpaired, one-tailed). Major mass isotopomers occurring due to ^{13}C labelling are shown as M+3 or M+6, M+0 denotes no labelling. **e**, Messenger RNA was extracted from wild-type, *Vil1-creER;Apc^{fl/fl}* and *Vil1-creER;Apc^{fl/fl};Kras^{G12D/+}* intestinal tissue 3–4 days after induction with tamoxifen. Analysis of SSP enzyme expression was performed using qRT–PCR (n = 6 mice per genotype, qRT–PCR performed in technical duplicate). Error bars are s.e.m. **f**, *Vil1-creER;Apc^{fl/+};Kras^{G12D/+}* mice were placed on SG-free or control diet at 6–8 weeks of age, then induced with tamoxifen after two weeks. Survival to clinical end point is shown. n, number of mice per cohort; MS, median survival in days. P value calculated by Mantel–Cox test from day of induction. See Source Data.

We show that dietary limitation of SG can be effective in the treatment of some cancers, although whether dietary SG restriction would change serum or tumour amino acid levels in humans remains unknown. Combination of diet with agents that increase ROS is predicted to increase the therapeutic response. While elevation of SSP enzyme expression following Kras activation will make tumours less responsive to serine starvation treatment, the overall sensitivity of tumour cells to serine depletion will depend on the combinatorial effect of multiple genetic alterations. So although activation of Myc (directly or following Apc loss) can enhance SSP enzyme expression, the *Eμ-Myc* lymphoma model remained sensitive to SG starvation. In this context, mutation of Kras further enhanced SSP expression and increased resistance to the SG-free diet. By contrast, despite carrying activated Kras, HCT116 cells remain partially sensitive to SG depletion—a dependency that is further exacerbated by loss of p53 (ref. 7). A role for other tumour associated changes has recently been demonstrated in a study showing LKB1 deletion enhances activation of the SSP[35]. We therefore anticipate that while individual genetic alterations can give an indication of the sensitivity of cancers to SG limitation, the final response will be influenced by both tissue of origin[36] and its wider genetic landscape.

Methods

Cell lines and cell culture

HCT116 cells were obtained from ATCC and authenticated using Promega GenePrint 10. iKras cells (iKras1, iKras3, AK196) were supplied by R. DePinho[30] (University of Texas MD Anderson Cancer Center). Cell culture media were purchased from Gibco (Thermo Fisher Scientific), product numbers are shown in parentheses. iKras (DMEM - 21969) and HCT116 cells (RPMI-1640 - 31870) were maintained in the stated media supplemented with 10% FBS (10270), penicillin–streptomycin and amphotericin with L-glutamine at final concentration of 2 mM. Stock iKras cells were grown in the presence of doxycycline 2 µg ml^{-1} (Kras-ON) and in medium with/without doxycycline (Kras-ON/OFF) for experiments. Cells were maintained in 37 °C, 5% CO_2 humidified incubators. Cultured cells were routinely tested for mycoplasma using Mycoalert detection kit (Lonza).

Proliferation assays

iKras cells were seeded in complete DMEM medium plus doxycycline 2 µg ml^{-1} in 24-well plates and allowed to adhere overnight. Cells were then washed with PBS and received either assay medium with or without SG, with or without doxycycline 2 µg ml^{-1}. HCT116 cells (2.5×10^4 per well) were seeded in complete RPMI medium in 24-well plates and allowed to adhere overnight. Cells were then washed with PBS and received modified MEM medium supplemented with various concentrations of SG[7]. Medium was replaced with fresh medium every 24 h. Wells were counted (using Casy TT cell counter, Innovatis, Roche Applied Science) at the stated time points, using a 'time = 0' plate to calculate relative cell number from time of medium change.

Tumour organoid culture

Vil1-creER;Apc$^{fl/fl}$ and *Vil1-creER;Apc$^{fl/fl}$;Kras$^{G12D/+}$* mice were induced with 80 mg kg^{-1} tamoxifen at 8–10 weeks, and crypts were isolated from intestinal tissue 3–4 days after induction (1 day before humane clinical end point in this model). Organoids were grown in Advanced DMEM/F-12 (ADF), supplemented with 2 mM glutamine, 1% penicillin–streptomycin solution, 0.1% AlbuMAX I BSA, 10 mM HEPES (all Gibco, Thermo Fisher Scientific). Adenomatous small intestine tissue was excised and cut into smaller pieces and washed five times with ice-cold PBS. Pieces were incubated in 5 mM EDTA for 10 min at 4 °C on a roller. Crypts were washed two times with ice-cold PBS to remove EDTA and incubated in 10× trypsin for 30 min at 37 °C. The crypt-enriched supernatant was collected and washed approximately five times with 5 ml ADF through mechanical pipetting. Crypts were pelleted via centrifugation at 1,200 r.p.m. for 5 min. Crypts were re-suspended in growth-factor-reduced Matrigel (BD Biosciences) and 20 µl was plated per well in a 12-well plate. Matrigel was allowed to solidify for 30 min in a 37 °C incubator before appropriate ADF was added supplemented with 0.05 µg ml^{-1} EGF and 0.1 µg ml^{-1} noggin (Total volume per well 1 ml). Crypts were split by harvesting in ice-cold PBS and spun down at 600 r.p.m. for 3 min. Supernatant was aspirated and the pellet dissociated with 100 µl ice-cold PBS using mechanical pipetting. Five millilitres of PBS was added to tube and spun down at 600 r.p.m. for 3 min, repeated until supernatant was clear of debris. The final crypt pellet was re-suspended with growth-factor-reduced Matrigel and plated as before. For SG starvation, amino-acid-free Advanced DMEM/F-12 (Gibco, Thermo Fisher Scientific) was used to construct assay medium for organoids with or without SG (0.2 mM), containing all other amino acids. For LCMS analysis organoids were grown in 12-well plates in complete medium for three days. Medium was aspirated and organoids were washed with PBS. The medium was replaced with

glucose-free Advanced DMEM/F-12 (Gibco, Thermo Fisher Scientific) supplemented with 15 mM $^{13}C_6$-glucose (CK-Gas/Cambridge Isotopes). After five hours media was aspirated, organoids were briefly washed in PBS and metabolites were extracted as described below.

Organoid imaging

Organoids were seeded in the stated media with or without metformin/daunorubicin (both from Sigma-Aldrich) and allowed to grow for two days. Images for size quantification (performed using ImageJ software) were taken using a light microscope then organoids were fixed in 4% paraformaldehyde. ROS damage was assessed by immunostaining organoids with anti-malondialdehyde (MDA) (Abcam, ab6463), with Alexa Fluor 594 secondary antibody (Thermo Fisher Scientific). Images were captured on an Olympus FV1000 inverted laser scanning confocal microscope and MDA staining was quantified using ImageJ software.

Liquid chromatography–mass spectrometry (LC–MS)

Samples were prepared in cold (−20 °C) lysis solvent (LS) consisting of methanol, acetonitrile, and H_2O (50:30:20). Serum (isolated from terminal bleeds and stored at −80 °C) samples of 10 µl were added to 490 µl of LS and vortexed, precipitated protein was cleared by centrifugation (15,000 r.p.m. for 10 mins at 4 °C). Organoid extracts were prepared by briefly washing wells with excess PBS then adding 250 µl LS per well and placing on a rocking shaker at 4 °C for 10 min, LS was removed from wells (without mechanical disruption of organoids/Matrigel) and then vortexed and cleared by centrifugation. Tissue samples were snap-frozen and stored at −80 °C. Prior to lysis, frozen samples were weighed. Tissues were then homogenized in 1 ml cold LS using a Precellys homogenizer (Bertin Technologies) or a TissueLyser II (Qiagen). Lysates were cleared of protein by centrifugation and lysate concentrations normalized post-homogenization with LS to 10 mg ml^{-1}based on original tissue weight.

Extracts were analysed on an LC–MS platform consisting of an Accela 600 LC system and an Exactive mass spectrometer (Thermo Scientific). Two LC methods were applied for metabolite separation before MS detection. Method 1 employed a SeQuant ZIC-pHILIC column (2.1 mm × 150 mm, 5 µm) (Merck) with the mobile phase mixed by A = ammonium carbonate 20 mM (adjusted to pH 9.4) and B = acetonitrile. A gradient program starting at 20% of A and after 2 min linearly increasing to 80% at 17 min was used followed by washing and re-equilibration steps. The total run time of the method 1 was 25 min. Method 2 employed a ZIC-HILIC column (4.6 mm × 150 mm, 3.5 µm) (Merck) with the mobile phase mixed by A = water with 0.1% formic acid (v/v) and B = acetonitrile with 0.1% formic acid. A gradient program starting at 20% of A and linearly increasing to 80% at 30 min was used followed by washing and re-equilibration steps. The total run time of method 2 was 46 min. The LC stream was desolvated and ionized in the HESI probe. The Exactive mass spectrometer was operated in full-scan mode over a mass range of 75–1,000 m/z at a resolution of 50,000 with polarity switching. LC–MS quantification of serine and glycine was achieved with six-point standard curves using ^{13}C–^{15}N-labelled amino acids (Sigma-Aldrich) diluted in a relevant matrix matched to the analytical sample. The raw data was analysed by LCquan (Thermo Scientific) and MZMine 2.10 for metabolite identification and quantification.

Unbiased metabolomics

Raw LC–MS data was converted into mzML files using ProteoWizard and imported into MZMine 2.10 for peak extraction and sample alignment. The generated.csv file was imported into an in-house macro (Microsoft Excel 2010) for metabolite identification and removal of background signals. The detailed procedure and setting parameters are previously described[37]. SIMCA 14 (Umetrics) was used for multivariate analysis. The S-plots were produced in OPLS-DA (orthogonal partial least squares discriminant analysis) models for targeting the most influential metabolites.

Diets

From weaning, mice received 'normal chow' (Rat and Mouse Breeder and Grower, 801730, Special Diet Services, SDS, UK) and water *ad libitum*. On normal chow, dietary amino acids are derived from whole proteins contained in the raw ingredients (wheat, wheatfeed, barley, de-hulled extracted toasted soya, maize and fish meal), with a small amount of purified lysine added as a supplement. Two sets of experimental diets were used, both based on Baker Purified Amino Acid Diet[38] from TestDiet (Richmond, IN): 'Diet 1-Control' contained all essential amino acids plus serine, glycine, glutamine, arginine, cystine, and tyrosine; 'Diet 1-SG-free' was the same as Diet 1-Control, but without serine and glycine, with the other amino acid levels increased proportionally to achieve the same total amino acid content. These 'Diet 1' formulations were used previously[7]. 'Diet 2-Control' contained all essential amino acids plus serine, glycine, glutamine, arginine, cystine, tyrosine, alanine, proline, glutamate and asparagine; 'Diet 2-SG-free' was the same as Diet 2-Control, but without serine and glycine, with the other amino acid levels increased proportionally to achieve the same total amino acid content. 'Diet 2' formulations were used for the *Eµ-Myc;Tigar* experiment (Fig. 2f). All other cohorts received the previously published Diet 1 formulations.

GEMMs

All animal work was carried out in line with the Animals (Scientific Procedures) Act 1986 and the EU Directive 2010 (PPLs 60/4181, 70/8645 and 70/8646) and was sanctioned by the local ethical review process (University of Glasgow). *Mus musculus* cohorts were housed in a barrier facility proactive in environmental enrichment. Mice were genotyped by Transnetyx (Cordova, Tennessee, USA). The *Eµ-Myc* (ref. 9), *Apc^Min/+* (refs 39, 40), *Lgr5-creER;Apc^fl/fl* (ref. 41) *Vil1-creER;Apc^fl/fl*(ref. 42) *Vil1-creER;Apc^fl/+;LSL-Kras^G12D*, *Pdx1-cre;LSL-Kras^G12D/+;Trp53^fl/+* and *Pdx1-cre;LSL-Kras^G12D/+;LSL-Trp53^R172H/+* (refs 27, 28) alleles/models have been described previously. Mixed male and female populations were used for each genotype. The number of mice (or number of samples from individual mice) is shown in each figure or its legend. *Eµ-Myc*, and *Apc^Min/+* mice were at least 20 generations C57BL/6J (BL6). *Eµ-Myc;Tigar^-/-* mice were a mixed strain but at least 50% C57BL/6J. Pancreatic (PDAC) cohorts were on a mixed strain background but all cohorts consisted of litter-matched controls. Mice were put on the appropriate diet at the following times: *Eµ-Myc* (BL6) 60 days post-natal, *Eµ-Myc;Tigar^-/-* 55 days post-natal, *Apc^Min/+*80 days post-natal, *Lgr5-creER;Apc^fl/fl* 7 days post-induction, *Pdx1-cre;Kras^G12D/+;Trp53^fl/+* or *Pdx1-cre;Kras^G12D/+;Trp53^R172H/+* 60 days post-natal. Recombination in *Lgr5-creER* mice was induced with two intraperitoneal injections of 120 mg kg⁻¹ tamoxifen, with a day's rest between the injections. For the phenformin experiment, *Eµ-Myc* mice were gavaged daily with 100 mg kg⁻¹mouse body weight, starting the same day as the diet change. For the metformin experiment, *Apc^Min/+* mice were given 200 mg kg⁻¹ per day in their drinking water, starting five days after the diet change. *Vil1-creER;Apc^fl/+;Kras^G12D/+* mice (C57Bl/6J N10) were placed on experimental diet at 6–8 weeks of age, kept on diet for two weeks, and then

induced with a single intraperitoneal injection of tamoxifen (80 mg kg^{-1}). Intestines were fixed in methacarn (4:2:1 ratio of methanol, chloroform, acetic acid) to facilitate scoring of tumour number and measurement of tumour area (width × length for each adenoma). Apart from $n = 6$ $Apc^{min/+}$ mice, which were taken at a temporal end point for BrdU and caspase staining, all other GEMMs were killed at humane clinical end point.

Sample sizes for mouse studies were estimated from previous experience with these models where potential differences in survival are tested by Mantel–Cox (log rank) analysis. No statistical methods were used to predetermine sample size. After data was collected for the first experimental groups (for example, $E\mu$-Myc and $Apc^{Min/+}$ on diet only, Fig. 1a, b) subsequent groups were reduced in size to minimize animal numbers used (for example, phenformin and metformin treatment groups, Fig. 2a, b). In all experiments mice with overt phenotype at time of enrolment into the study were excluded (that is, not enrolled): for example, enlarged lymph nodes or signs of enlarged thymus in the $E\mu$-Myc cohorts, anaemia in the $Apc^{Min/+}$ cohorts. Animals that died as a result of illness unrelated to tumour(s) were included as censored observations. Mice were allocated into the experimental groups according to a randomized block design: as mice became available through breeding, they were split into blocks based on gender and then randomly assigned to a treatment arm. Care was taken to keep the male/female ratio similar in order to remove gender as a potential source of variability. The investigator allocating mice to the experimental groups and collecting the end point data was not blinded.

In vivo $^{13}C_3$–$^{15}N_1$-serine uptake

$Pdx1$-$cre;Kras^{G12D/+};Trp53^{R172H/+}$ mice, non-Cre-expressing isogenic control mice with normal pancreas and $Apc^{Min/+}$ mice were injected in the tail vein with 100 µl of 100 mM $^{13}C_3$–$^{15}N_1$-serine (CKGas/Cambridge Isotopes) and left for two hours. PDAC/normal pancreas/adenoma/normal intestine tissues were excised and snap-frozen on dry ice for LC–MS analysis.

Xenografts/allografts in mice

HCT116 cells were implanted by bilateral subcutaneous injections ($3 × 10^6$ cells per flank) into Crl:CD1-$Foxn1^{nu}$ (CD1-Nude) female mice (Charles River, UK). Mice were maintained on normal chow diet and monitored daily until visible, measurable tumours had formed. Tumour-bearing mice were placed onto control or SG-free diet, tumours were measured with callipers three times per week, any opposing flank tumours, which developed subsequent to diet change were excluded from the analysis. Average tumour volumes are plotted for the first five weeks on diet. Tumour volumes were calculated using the formula:
$$\text{volume} = \frac{\text{length} \times \text{width}^2}{2}$$

$E\mu$-Myc lymphoma cells were isolated from tumour bearing lymph nodes of mixed background $E\mu$-Myc mice by FACS. These cells were initially expanded in cell culture with irradiated mouse embryonic fibroblasts (MEFs) and passaged until they could grow independently. Culture medium was DMEM/F-12 (Gibco, Thermo Fisher Scientific) supplemented with 10% FBS, 50 µM β-mercaptoethanol, penicillin, streptomycin, gentamycin and amphotericin. Cells were implanted by bilateral subcutaneous injections ($5 × 10^5$ cells per flank) into CD1-Nude female mice (Charles River, UK). Mice were maintained on normal chow diet and monitored daily until visible, measurable tumours (~5 mm) had formed. Tumour-bearing mice were placed onto control or SG-free diets, tumours were measured with callipers every 2 or 3 days. Once the first mouse in the cohort reached clinical end point (maximum permitted tumour size) all mice in the cohort were killed and tumours

removed (this occurred after 6 days on diet). Tumours were fixed in formalin, paraffin-embedded and sections cut for histology.

All experiments adhered strictly to the limits of the project licence authority (maximum permitted tumour size of 15 mm or ulceration), at which point the animals were humanely killed. In none of the experiments were these limits exceeded.

BrdU and caspase staining and necrosis quantification

Two hours before death, mice were injected with 250 μl of cell proliferation labelling reagent containing BrdU (RPN201, Amersham/GE Heathcare). Antibodies used: cleaved caspase 3 ASP-175 (Cell Signaling Technology, 9661), anti-BrdU (BD Biosciences, 347580) and EnVision anti-rabbit (Dako, K4003). Tissue sections were counterstained with haematoxylin Z (CellPath). Stained slides were scanned using a Leica SCN400F scanner and analysed using HALO Image analysis software (Indica Labs). For *Eμ-Myc* tumours cell number and BrdU and caspase staining were quantified across the whole tumour with necrotic areas excluded. For *Apc^Min/+* mice, single cross-sections of the entire small intestine were analysed, adenomas were manually identified and cell number, caspase and BrdU staining in each adenoma was quantified and averaged for each mouse. Necrosis was quantified using haematoxylin and eosin (H&E)-stained whole tumour cross-sections, necrotic areas were manually defined using HALO software and total necrotic versus non-necrotic surface area were calculated.

Glucose and lactate quantification

Serum (from terminal blood samples) from mouse cohorts were analysed for glucose and lactate levels using a YSI 2950 Biochemistry Analyser (Xylem) according to the manufacturer's instruction.

Macropinocytosis assay

Analysis of macropinocytosis was based on a previously descried protocol[31]. Initially, iKras cells were grown with (Kras-ON) or without (Kras-OFF) doxycycline for 48 h. Cells were then seeded onto glass coverslips in medium with or without doxycycline and with or without SG. After 24 h the medium was replaced with matched medium lacking FBS and left for a further 16 h. Finally, medium was replaced with matched medium containing 10% FBS and tetramethylrhodamine-labelled dextran (TMR-dextran, Thermo Fisher Scientific) particles (0.5 mg ml^{-1}). After 30 min with dextran, cells were washed with PBS and fixed in 4% formaldehyde. Cells were counterstained with DAPI and green Whole Cell Stain (Thermo Scientific) and mounted in Vectasheild Hardset (Vector Laboratories). Images were captured on an Olympus FV1000 inverted laser scanning confocal microscope and dextran uptake was quantified using ImageJ/Fiji image analysis software.

Western blot

Western blots on cells were performed as described previously[6, 7, 43]. In brief, whole-cell protein lysates were prepared in RIPA buffer supplemented with complete protease inhibitors (Roche), sodium orthovanadate, and sodium fluoride (both Sigma-Aldrich). Tissue samples were lysed in RIPA buffer supplemented with protease and phosphatase inhibitor cocktail (Pierce/Thermo Scientific) using a TissueLyser II (Qiagen). Lysates were cleared by centrifugation and separated using precast

4–12% 'NuPAGE' or 'Bolt' gels (Invitrogen, Life Technologies) and transferred to nitrocellulose membranes. Proteins were detected and quantified using a Li-Cor Odyssey Infrared scanner and software (Li-Cor Biosciences). Secondary antibodies for the relevant species were IRDye680 and IRDye800 conjugated (Li-Cor Biosciences). Primary antibodies used were: PHGDH (Sigma-Aldrich Life Science, HPA021241), PSAT1 (Novus Biologicals, NBP1-32920), PSPH (Santa Cruz, sc-98683), Actin I-19-R (Santa-Cruz, sc-1616-R), pERK (phospho-p44/p42 MAPK (Erk1/2) (Thr202/Tyr204)) (Cell Signalling Technology 9101), AMPKa1 (R&D Systems, AF3197) and phospho-AMPK T172 (Cell Signalling Technology 2535).

qRT–PCR

RNA was extracted from iKras cells and organoids using RNeasy kit with DNase (both Qiagen) to remove DNA. qRT–PCR was performed as described previously[7] using an Applied Biosystems 7500 Fast Real-Time PCR system with SYBR Green master mix (Applied Biosystems). Intestinal tissues were obtained from 6–8-week-old wild-type, *Vil1-creER;Apc^fl/fl* or *Vil1-creER;Apc^fl/fl;LSL-Kras^G12D/+* mice. The mice were sampled 3–4 days after induction with tamoxifen (80 mg kg^{-1}). RNA from intestinal tissue was extracted using a Qiagen RNeasy Mini Kit (Qiagen) according to the manufacturer's instructions. A DyNAmo SYBR Green 2-step qPCR kit (Finnzymes) was used to reverse-transcribe 1 μg of RNA in a reaction volume of 20 μl. Finally, qPCR was carried out using a MesaGreen kit according to the manufacturer's intructions (Eurogentec) and a Chromo4 thermocycler (Biorad). Expression results obtained were normalized to β-actin levels. Mouse SSP primers are previously published[44] sequences (5'–3'): mouse *Phgdh* F: TGGCCTCGGCAGAATTGGAAG; mouse *Phgdh* R: TGTCATTCAGCAAGCCTGTGG T; mouse *Psat1*-For GATGAACATCCCATTTCGCATTGG; mouse *Psat1* R: GCGTTATACAGAGAGGCACGAA TG; mouse *Psph* F: GAGATGGAGCTACGGACATGGAAG; mouse *Psph* R: CTCCTCCAGTTCTCCCAGCAGCT C. Sequences synthesized and purified by Eurofins MWG Operon. Mouse *Actb* was purchased from Primer Design (HK-SY-mo-900 ACTB).

Statistics

Statistical comparisons for survival data were calculated with Graphpad Prism (v6) software using Mantel–Cox (Log Rank) test. *t*-tests were either performed using Microsoft excel (v14.6.1) or Graphpad Prism (v7). Type 1/paired (for example, samples taken from the same animal) and type 2/unpaired (for example, samples taken from different animals) *t*-tests were used. Where no prediction was made about the direction of potential difference a two-tailed *t*-test was used (for example, across all amino acid levels in serum samples, Fig. 1c and Extended Data Fig. 2a). Where pre-existing data supported a prediction in the direction of difference between samples a one-tailed *t*-test was used (for example, *de novo* serine synthesis, Fig. 4c). Where data presented is the mean of individual data points, error bars are s.d., where data are a mean of means, error bars are s.e.m. In each instance the relevant type of *t*-test or error bar is specified in the figure legend. Where *t*-tests were performed with multiple comparisons, *P* values were corrected using the Holm–Sidak method using GraphPad Prism (v7) software.

Data availability

Data are available in Supplementary Information and on request from the authors.
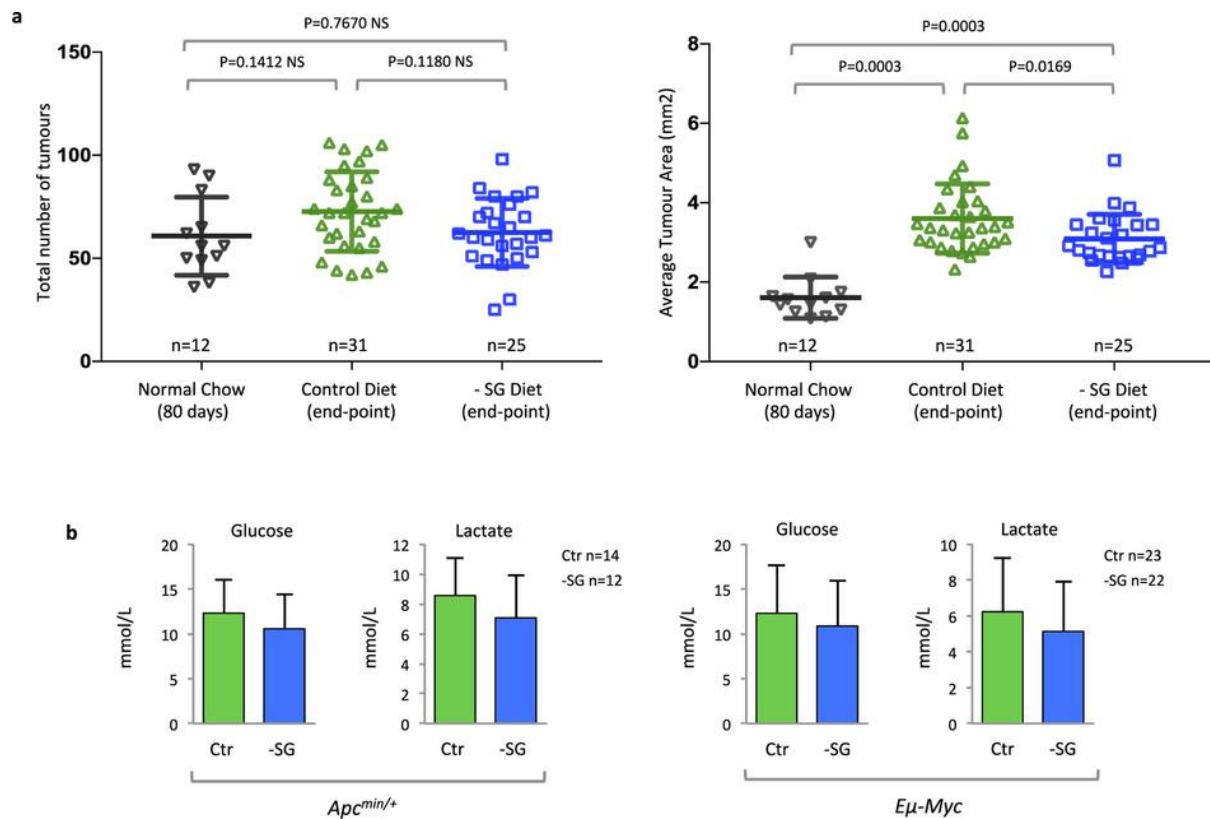
Acknowledgements

References

1. Locasale, J. W. Serine, glycine and one-carbon units: cancer metabolism in full circle. Nat. Rev. Cancer 13, 572–583 (2013).

2. Locasale, J. W. & Cantley, L. C. Genetic selection for enhanced serine metabolism in cancer development. Cell Cycle 10, 3812–3813 (2011).

3. Possemato, R. et al. Functional genomics reveal that the serine synthesis pathway is essential in breast cancer. Nature 476, 346–350 (2011).

4. Snell, K. Enzymes of serine metabolism in normal and neoplastic rat tissues. Biochim. Biophys. Acta 843, 276–281 (1985).

5. Jain, M. et al. Metabolite profiling identifies a key role for glycine in rapid cancer cell proliferation. Science 336, 1040–1044 (2012).

6. Labuschagne, C. F., van den Broek, N. J., Mackay, G. M., Vousden, K. H. & Maddocks, O. D. Serine, but not glycine, supports one-carbon metabolism and proliferation of cancer cells. Cell Reports 7, 1248–1258 (2014).

7. Maddocks, O. D. et al. Serine starvation induces stress and p53-dependent metabolic remodelling in cancer cells. Nature 493, 542–546 (2013).

8. Gravel, S. P. et al. Serine deprivation enhances antineoplastic activity of biguanides. Cancer Res. 74, 7521–7533 (2014).

9. Adams, J. M. et al. The c-myc oncogene driven by immunoglobulin enhancers induces lymphoid malignancy in transgenic mice. Nature 318, 533–538 (1985).

10. Shoemaker, A. R., Moser, A. R. & Dove, W. F. N-ethyl-N-nitrosourea treatment of multiple intestinal neoplasia (Min) mice: age-related effects on the formation of intestinal adenomas, cystic crypts, and epidermoid cysts. Cancer Res. 55, 4479–4485 (1995).

11. Chaneton, B. et al. Serine is a natural ligand and allosteric activator of pyruvate kinase M2. Nature 491, 458–462 (2012).

12. Ye, J. et al. Pyruvate kinase M2 promotes de novo serine synthesis to sustain mTORC1 activity and cell proliferation. Proc. Natl Acad. Sci. USA 109, 6904–6909 (2012).

13. Shackelford, D. B. et al. LKB1 inactivation dictates therapeutic response of non-small cell lung cancer to the metabolism drug phenformin. Cancer Cell 23, 143–158 (2013).

14. Quinn, B. J., Kitagawa, H., Memmott, R. M., Gills, J. J. & Dennis, P. A. Repositioning metformin for cancer prevention and treatment. Trends Endocrinol. Metab. 24, 469–480 (2013).

15. Wang, D. S. et al. Involvement of organic cation transporter 1 in hepatic and intestinal distribution of metformin. J. Pharmacol. Exp. Ther. 302, 510–515 (2002).

16. Reagan-Shaw, S., Nihal, M. & Ahmad, N. Dose translation from animal to human studies revisited. FASEB J. 22, 659–661 (2008).

17. Dowling, R. J. et al. Metformin pharmacokinetics in mouse tumors: implications for human therapy. Cell Metab. 23, 567–568 (2016).

18. Chandel, N. S. et al. Are metformin doses used in murine cancer models clinically relevant? Cell Metab. 23, 569–570 (2016).

19. Chakraborty, A., Chowdhury, S. & Bhattacharyya, M. Effect of metformin on oxidative stress, nitrosative stress and inflammatory biomarkers in type 2 diabetes patients. Diabetes Res. Clin. Pract. 93, 56–62 (2011).

20. Esteghamati, A. et al. Effects of metformin on markers of oxidative stress and antioxidant reserve in patients with newly diagnosed type 2 diabetes: a randomized clinical trial. Clin. Nutr. 32, 179–185 (2013).

21. Hou, X. et al. Metformin reduces intracellular reactive oxygen species levels by upregulating expression of the antioxidant thioredoxin via the AMPK–FOXO3 pathway. Biochem. Biophys. Res. Commun. 396, 199–205 (2010).

22. Wheaton, W. W. et al. Metformin inhibits mitochondrial complex I of cancer cells to reduce tumorigenesis. eLife 3, e02242 (2014).

23. Bensaad, K., Cheung, E. C. & Vousden, K. H. Modulation of intracellular ROS levels by TIGAR controls autophagy. EMBO J. 28, 3015–3026 (2009).

24. Bensaad, K. et al. TIGAR, a p53-inducible regulator of glycolysis and apoptosis. Cell 126, 107–120 (2006).

25. Cheung, E. C. et al. Opposing effects of TIGAR- and RAC1-derived ROS on Wnt-driven proliferation in the mouse intestine. Genes Dev. 30, 52–63 (2016).

26. Cheung, E. C., Ludwig, R. L. & Vousden, K. H. Mitochondrial localization of TIGAR under hypoxia stimulates HK2 and lowers ROS and cell death. Proc. Natl Acad. Sci. USA 109, 20491–20496 (2012).

27. Hingorani, S. R. et al. Trp53R172H and KrasG12D cooperate to promote chromosomal instability and widely metastatic pancreatic ductal adenocarcinoma in mice. Cancer Cell 7, 469–483 (2005).

28. Morton, J. P. et al. Mutant p53 drives metastasis and overcomes growth arrest/ senescence in pancreatic cancer. Proc. Natl Acad. Sci. USA 107, 246–251 (2010).

29. Son, J. et al. Glutamine supports pancreatic cancer growth through a KRAS-regulated metabolic pathway. Nature 496, 101–105 (2013).

30. Ying, H. et al. Oncogenic Kras maintains pancreatic tumors through regulation of anabolic glucose metabolism. Cell 149, 656–670 (2012).
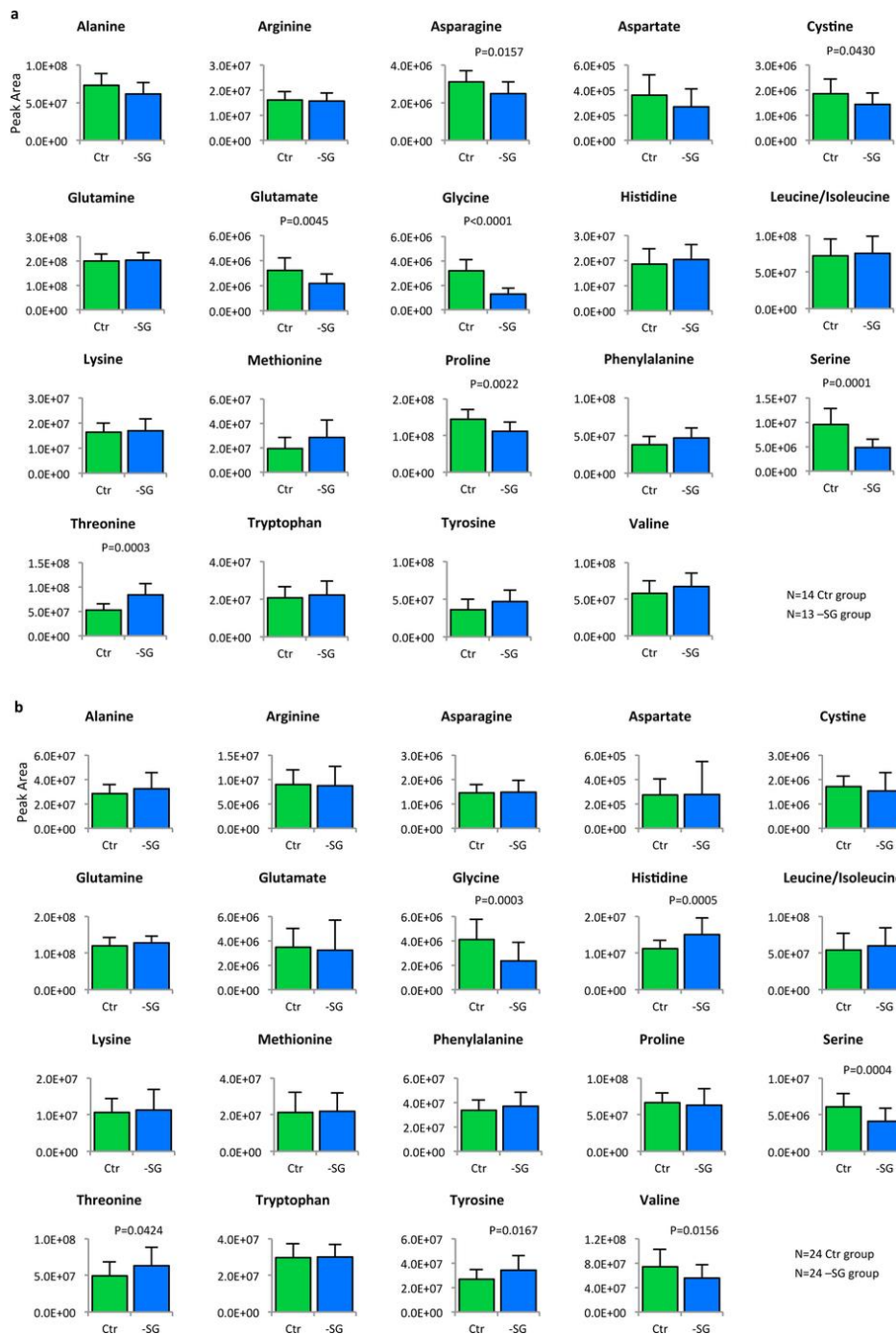
31. Commisso, C. et al. Macropinocytosis of protein is an amino acid supply route in Ras-transformed cells. Nature 497, 633–637 (2013).

32. Kamphorst, J. J. et al. Human pancreatic cancer tumors are nutrient poor and tumor cells actively scavenge extracellular protein. Cancer Res. 75, 544–553 (2015).

33. DeNicola, G. M. et al. Oncogene-induced Nrf2 transcription promotes ROS detoxification and tumorigenesis. Nature 475, 106–109 (2011).

34. DeNicola, G. M. et al. NRF2 regulates serine biosynthesis in non-small cell lung cancer. Nat. Genet. 47, 1475–1481 (2015).

35. Kottakis, F. et al. LKB1 loss links serine metabolism to DNA methylation and tumorigenesis. Nature 539, 390–395 (2016).

36. Mayers, J. R. et al. Tissue of origin dictates branched-chain amino acid metabolism in mutant Kras-driven cancers. Science 353, 1161–1165 (2016).

Extended Data Figure 1: Effect of SG-free diet on tumour burden in Apc^Min/+ mice, and on serum glucose and lactate in Apc^Min/+ and Eμ-Myc mice.


a, ApcMin/+ mice received normal chow until 80 days of age, then were transferred to either a control diet (containing SG) or a matched diet lacking serine and glycine (−SG) until clinical end point (intestinal-tumour-related survival). Post-mortem tumour measurement was performed on intestinal tissue at time of diet change (80 days) or clinical end point. P values calculated by t-test (unpaired, two-tailed, with correction for multiple comparisons). Diet-only tumour number data also shown in Fig. 2c. Diet-only tumour area data also shown in Extended Data Fig. 5b. See Source Data. b, ApcMin/+ and Eμ-Myc mice received normal chow until 80 and 60 days of age, respectively, then were transferred to either a control diet containing SG (Ctr) or a matched diet lacking SG (−SG) until clinical end point. Serum isolated from terminal bleeds was analysed with a YSI 2950 Biochemistry Analyser for glucose and lactate concentration. Error bars are s.d.

Extended Data Figure 2: Effect of SG-free diet on serum amino acids.

a, *Apc^Min/+* mice received normal chow until 80 days of age, then were transferred to either a control diet (containing SG) or a matched diet lacking serine and glycine (−SG) until clinical end point (intestinal-tumour-related survival). Post-mortem tumour measurement was performed on intestinal tissue at time of diet change (80 days) or clinical end point. *P* values calculated by *t*-test (unpaired, two-tailed, with correction for multiple comparisons). Diet-only tumour number data also shown in Fig. 2c. Diet-only tumour area data also shown in Extended Data Fig. 5b. See Source Data. **b**, *Apc^Min/+* and *Eμ-Myc* mice received normal chow until 80 and 60 days of age, respectively, then were transferred to either a control diet containing SG (Ctr) or a matched diet lacking SG (−SG) until clinical end point. Serum isolated from terminal bleeds was analysed with a YSI 2950 Biochemistry Analyser for glucose and lactate concentration. Error bars are s.d.

Extended Data Figure 3: SG starvation impedes the growth of established HCT116 tumours by decreasing intratumoural serine and glycine concentration.
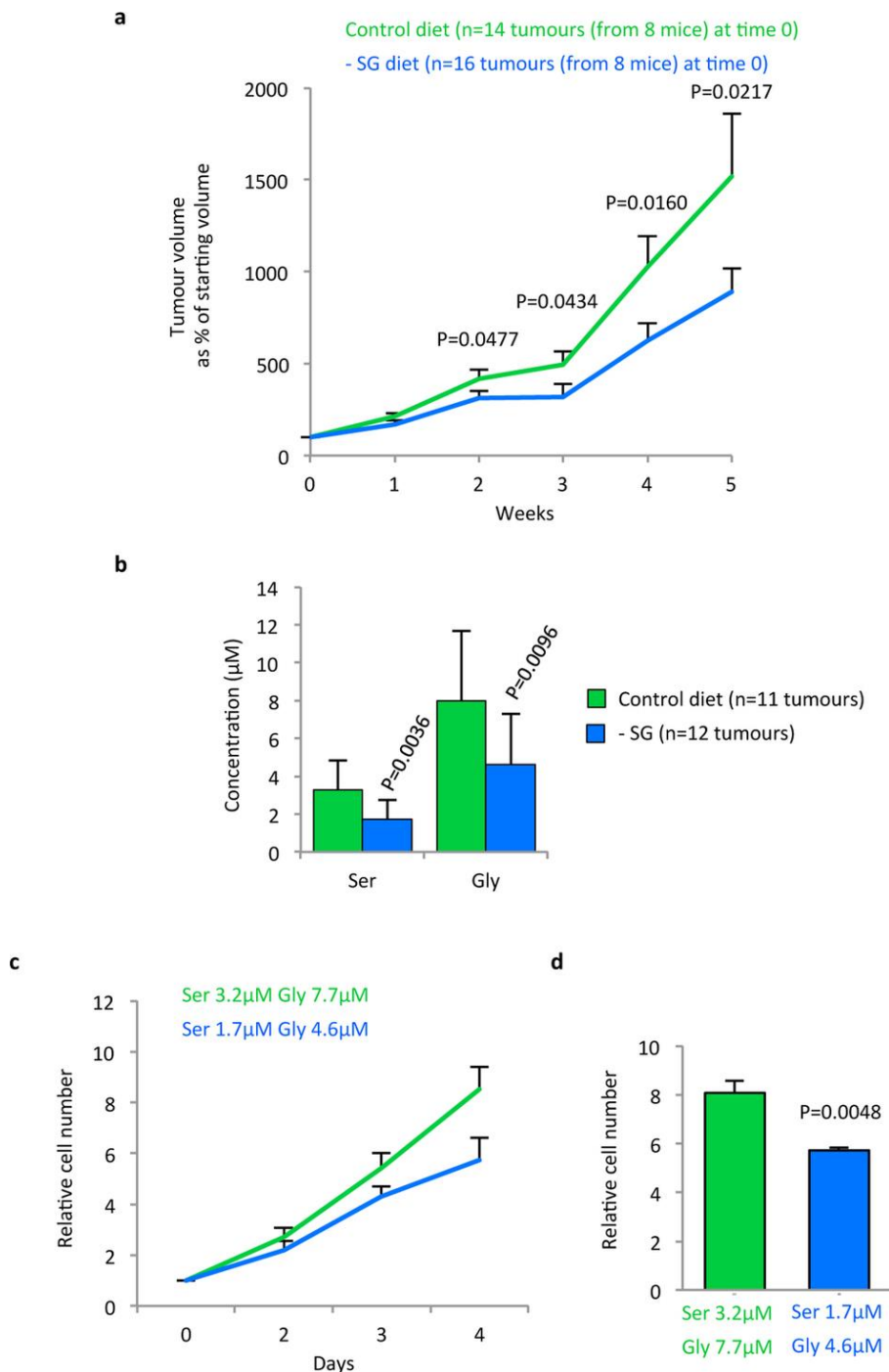
a, HCT116 cells were injected bilaterally (3×10^6 per flank, $n = 8$) and allowed to form tumours. Once tumours were visible and measurable by callipers mice were transferred to control diet or SG-free diet (−SG). Tumours were measured three times per week and average weekly tumour volume is plotted, error bars are s.e.m. *P* values were calculated by *t*-test (unpaired, one-tailed). See Source Data. **b**, HCT116 tumours (taken at clinical end point) were analysed by LC–MS for absolute concentration of SG (1–3 pieces of each tumour were analysed). Data are averages, error bars are s.d. *P* values were calculated by *t*-test (unpaired, one-tailed). **c**, HCT116 cells were grown *in vitro* (24-well plates) in the intratumoural SG concentrations displayed in **b**. Medium was replaced

every 24 h and cell counts were performed on the stated days. Data are averages of 12 replicate wells for each condition from an individual experiment, error bars are s.d. **d**, HCT116 cells were grown *in vitro* (24-well plates, 12 replicate wells for each condition) in the intratumoural SG concentrations displayed in **b**. Medium was replaced every 24 h and cell counts were performed after four days. Data are averages of three independent experiments, error bars are s.e.m. *P* values were calculated by *t*-test (unpaired, one-tailed).

*Extended Data Figure 4: Effect of SG-free diet on Apc$^{Min/+}$ and Eμ-Myc allograft tumours at temporal end points.*
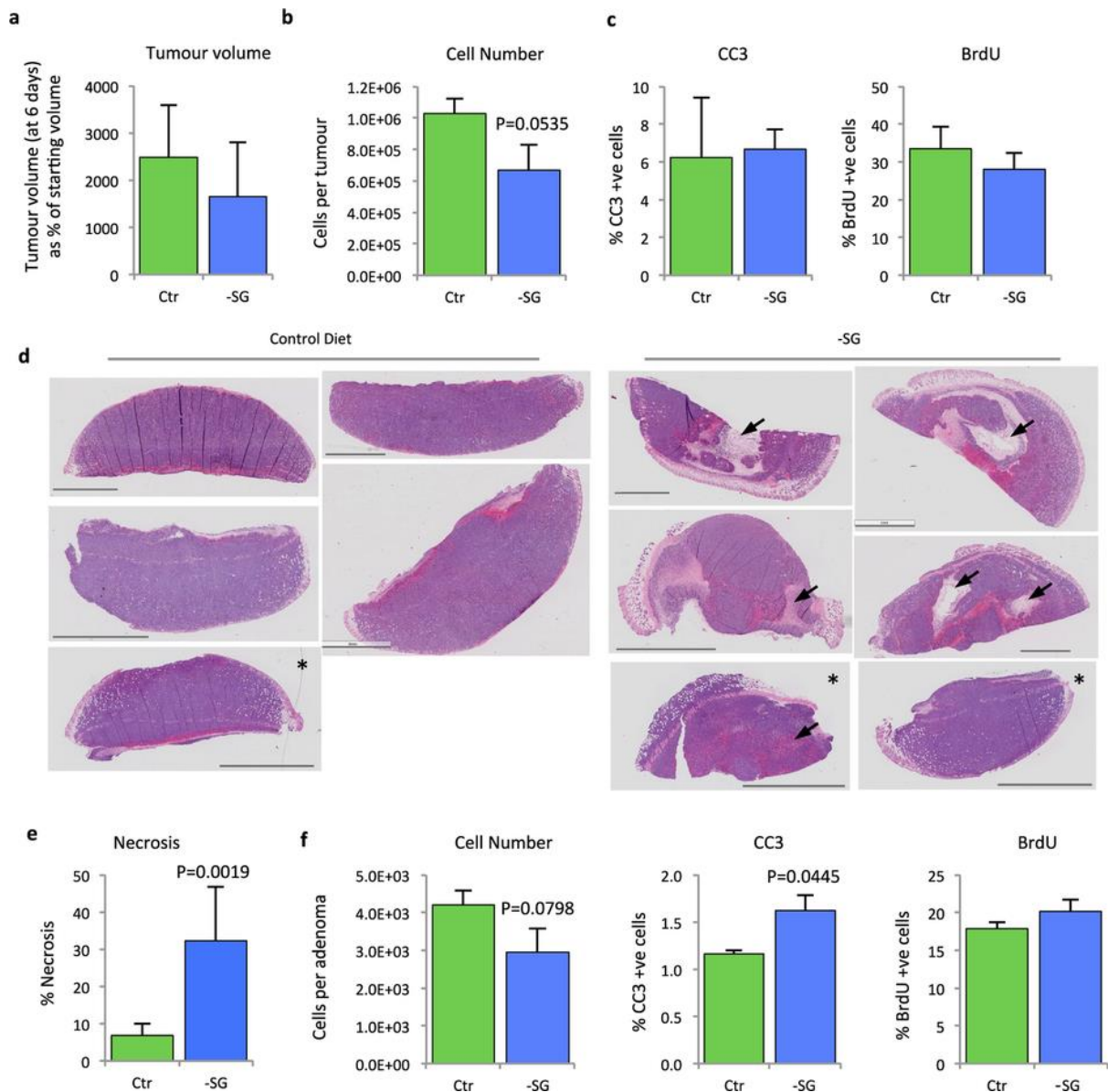
a, Lymphoma cells were isolated from *Eμ-Myc* mice and allowed to replicate in culture. Cells were injected subcutaneously (5 × 10^5 per flank) into nude mice and allowed to form tumours. Once tumours (Ctr, *n* = 4; −SG, *n* = 4) were visible and measurable, mice were transferred to control (Ctr) or SG-free diet (−SG). Mice were killed and tumours excised at single temporal end point (6 days on diet). Average tumour volume (as percentage of starting tumour volume) is shown, error bars are s.d. See Source Data. **b**, To assess cell number per subcutaneous *Eμ-Myc* tumour cross-section, two separate cell counts per tumour (using H&E-stained cross-sections) were performed and averaged, mean of means is shown, error bars are s.e.m. *P* values calculated by *t*-test (unpaired, one-tailed). **c**, Whole subcutaneous *Eμ-Myc* tumour tissue sections (Ctr, *n* = 3; −SG, *n* = 4) were immunostained for cleaved caspase-3 (CC3) and BrdU. Image analysis of non-necrotic regions of whole tumours allowed quantitative evaluation of the percentage of cleaved caspase-3-positive cells per tumour and the percentage of BrdU-positive cells per tumour. Data are averages, error bars are s.d. **d**, *Eμ-Myc* tumour (as described in **a**–**c** above) cross-sections were H&E stained, the scale bar for each

image is 4 mm, demonstrative necrotic regions marked with arrows. Additional tumour tissue sections (marked with asterisks) are included for comparison from tumours, which developed after diet change (these three tumours were measurable 2 days post diet change and were present for 4 days on diet before end point). **e**, Necrosis was quantified by image analysis of necrotic and non-necrotic surface area of H&E stains for the sections shown in **d**. Error bars are s.d. *P* value was calculated by *t*-test (unpaired, one-tailed; Ctr, *n* = 5; −SG, *n* = 6). **f**, *Apc*$^{Min/+}$ mice were placed on control diet (Ctr, *n* = 3) or SG-free diet (−SG, *n* = 3) at 80 days of age. At a single temporal end point (14 days on diet) mice were killed the small intestine was removed for histological analysis. Tissue sections were immunostained for cleaved caspase-3 and BrdU. Image analysis of whole intestines allowed quantitative evaluation of cell number per adenoma, percentage of CC3-positive cells and percentage of BrdU-positive cells per adenoma. Data are averages of all adenomas identified in each small intestine section, error bars are s.e.m., *P* values calculated by *t*-test (unpaired, one-tailed). For all analyses (**a–f**), *P* values below 0.1 are shown.

Extended Data Figure 5: Metformin treatment did not enhance the anti-tumour effect of SG-free diet in Apc^{Min/+} mice.

a
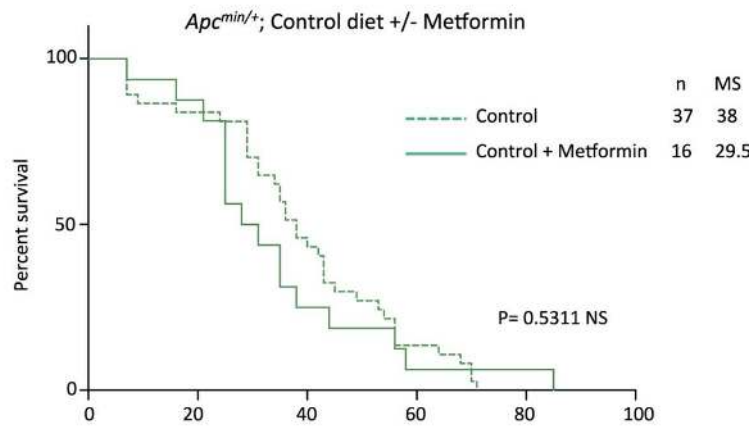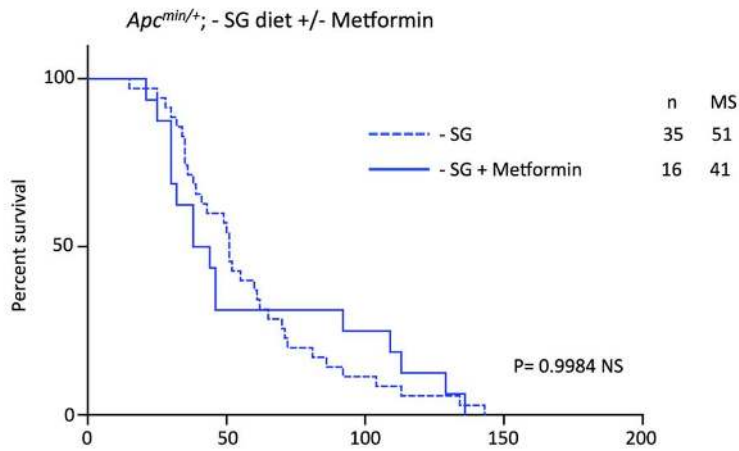
b
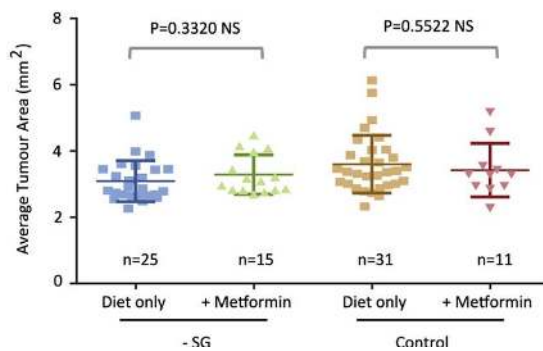
a, To clearly display the effect of metformin on survival of *Apc^{Min/+}* mice data from Fig. 2b is re-plotted on two separate graphs; *Apc^{Min/+}* mice were transferred to control or SG-free diet (−SG) at 80 days of age, then five days later received Metformin 200 mg kg^{-1} per day in drinking water. Intestinal-tumour-related survival calculated from change of diet. *n*, number of mice in cohort; MS, median survival in days. *P* values calculated by Mantel–Cox test. See Source Data. **b**, Post-mortem intestinal tumour measurement was performed on intestine tissue. *P* values calculated by *t*-test (unpaired, two-tailed). 'Diet only' data are replicated from Extended Data Fig. 1a. See Source Data.

Extended Data Figure 6: Quantification of metformin levels in Apc$^{Min/+}$ mice.
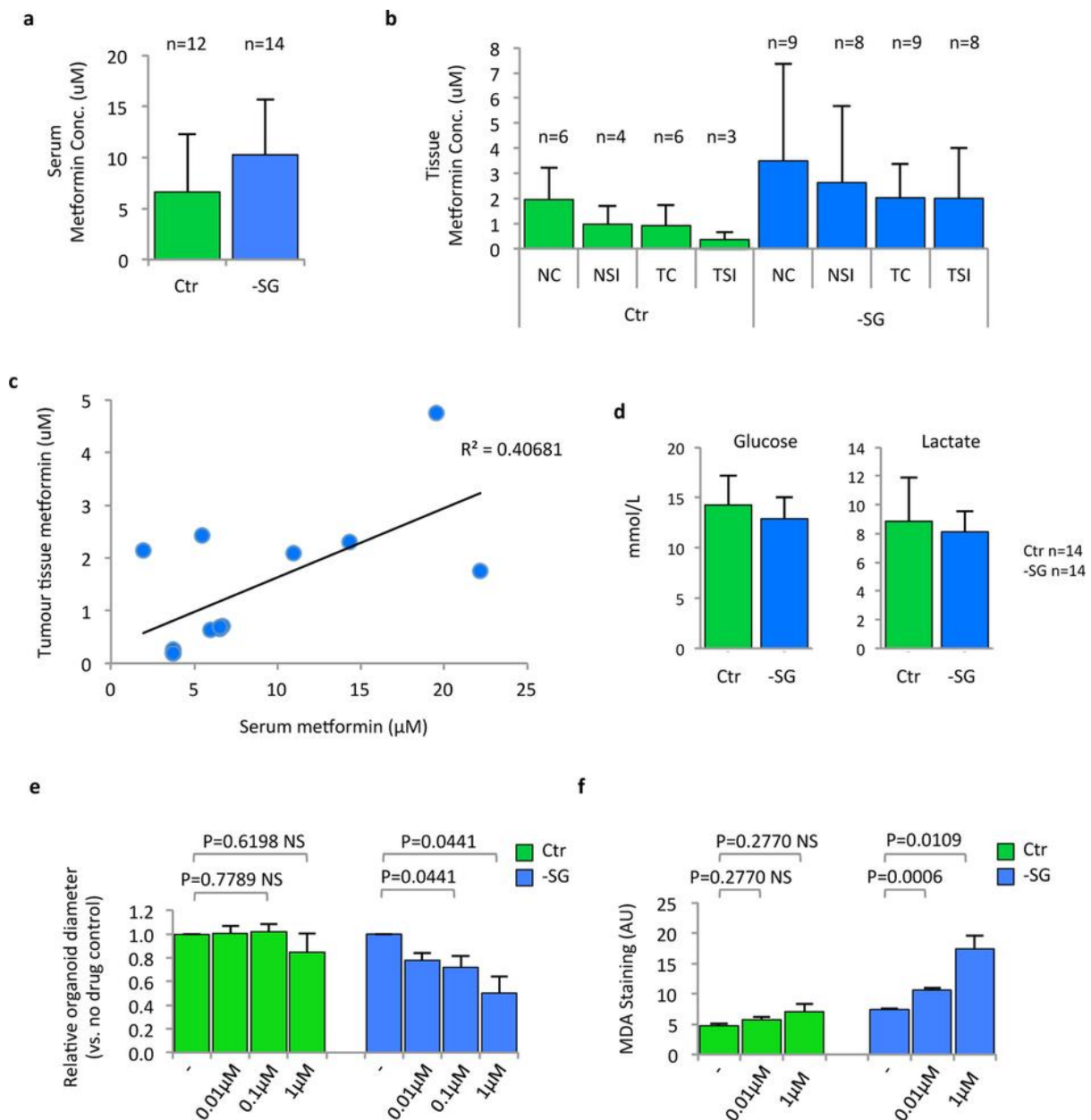
a, *Apc$^{Min/+}$* mice were transferred to control or SG-free diet (−SG) then received metformin 200 mg kg^{-1} per day in drinking water. Serum isolated from terminal bleeds was analysed by LC–MS. Error bars are s.d. **b**, Tissue samples from metformin-treated mice were analysed by LC–MS. NC, normal colon; NSI, normal small intestine; TC, tumour colon; TSI, tumour small intestine. Error bars are s.d. **c**, For mice where matching serum and tumour (small intestine or colon) tissue samples were available (Ctr diet, *n* = 7; −SG diet, *n* = 6), serum versus tumour metformin concentrations are plotted. Metformin concentrations were determined in all samples using a six-point calibration curve using the relevant biological matrix (tissue/serum). **d**, Serum from *Apc$^{Min/+}$* mice treated with metformin was analysed for glucose and lactate levels using a YSI 2950 Biochemistry Analyser. **e**, Intestinal tumour organoids derived from a *Vil1-creER;Apc$^{fl/fl}$* mouse were grown with or without serine and glycine and with or without daunorubicin at the stated concentrations for two days. Relative change (versus no drug control) in organoid diameter is plotted. Data are average of three independent experiments, error bars are s.e.m. **f**, *Vil1-creER;Apc$^{fl/fl}$* organoids were grown with or

without serine and glycine, and with or without daunorubicin for two days, then fixed and stained for malondialdehyde (MDA), data are average of three independent experiments, bars are s.e.m. *P* values calculated by *t*-test (unpaired, two-tailed, with correction for multiple comparisons).

Extended Data Figure 7: Effect of SG-free diet on serum amino acids in PDAC mice.
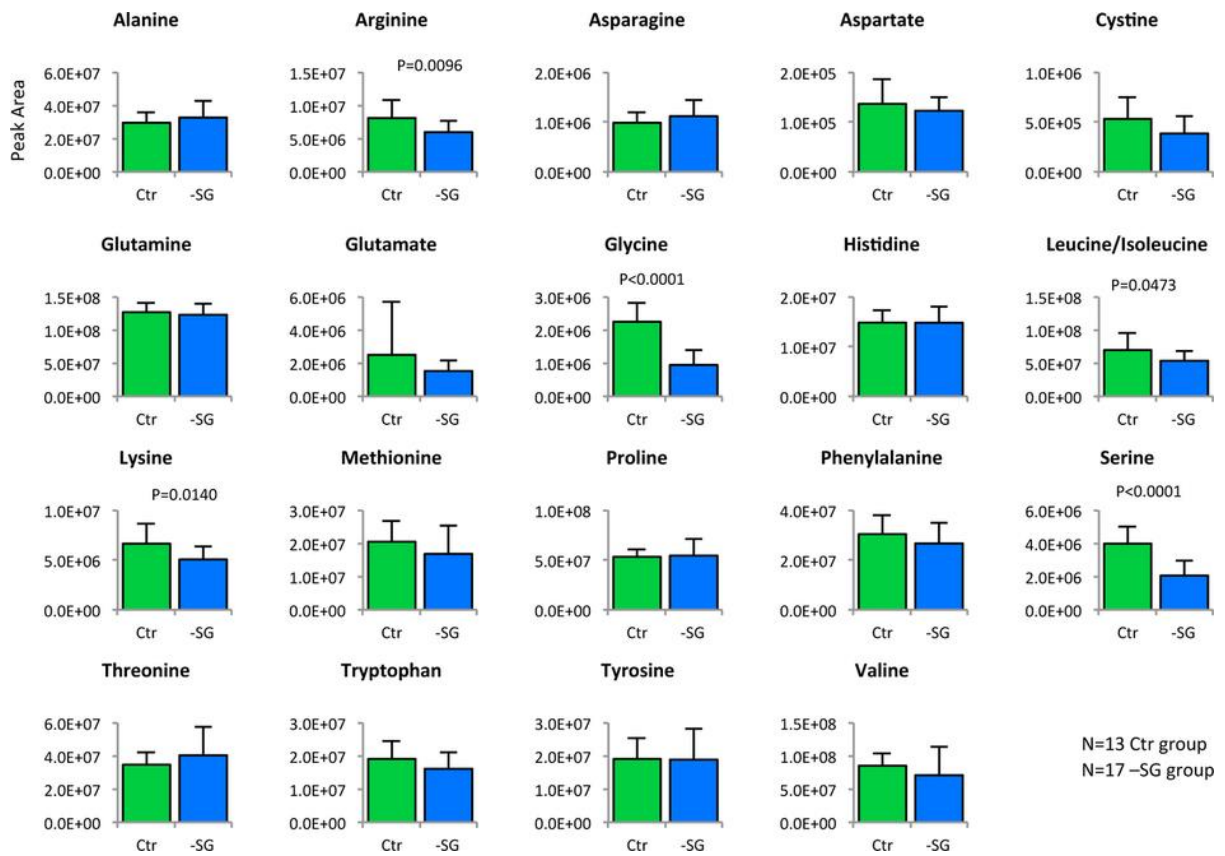
Pdx1-cre;Kras^G12D/+;Trp53^fl/+ mice received normal chow until 60 days of age, then were transferred to either a control diet containing serine and glycine (Ctr) or a matched diet lacking serine and glycine (−SG) until clinical end point. Serum isolated from terminal bleeds was analysed by LC–MS. Relative quantity of metabolites are shown (*y* axis = peak area). Error bars are s.d. *P* values were calculated for each amino acid by *t*-test (unpaired, two-tailed), *P* values <0.05 are shown.

Extended Data Figure 8: Effect of SG-free diet on PDAC mice.
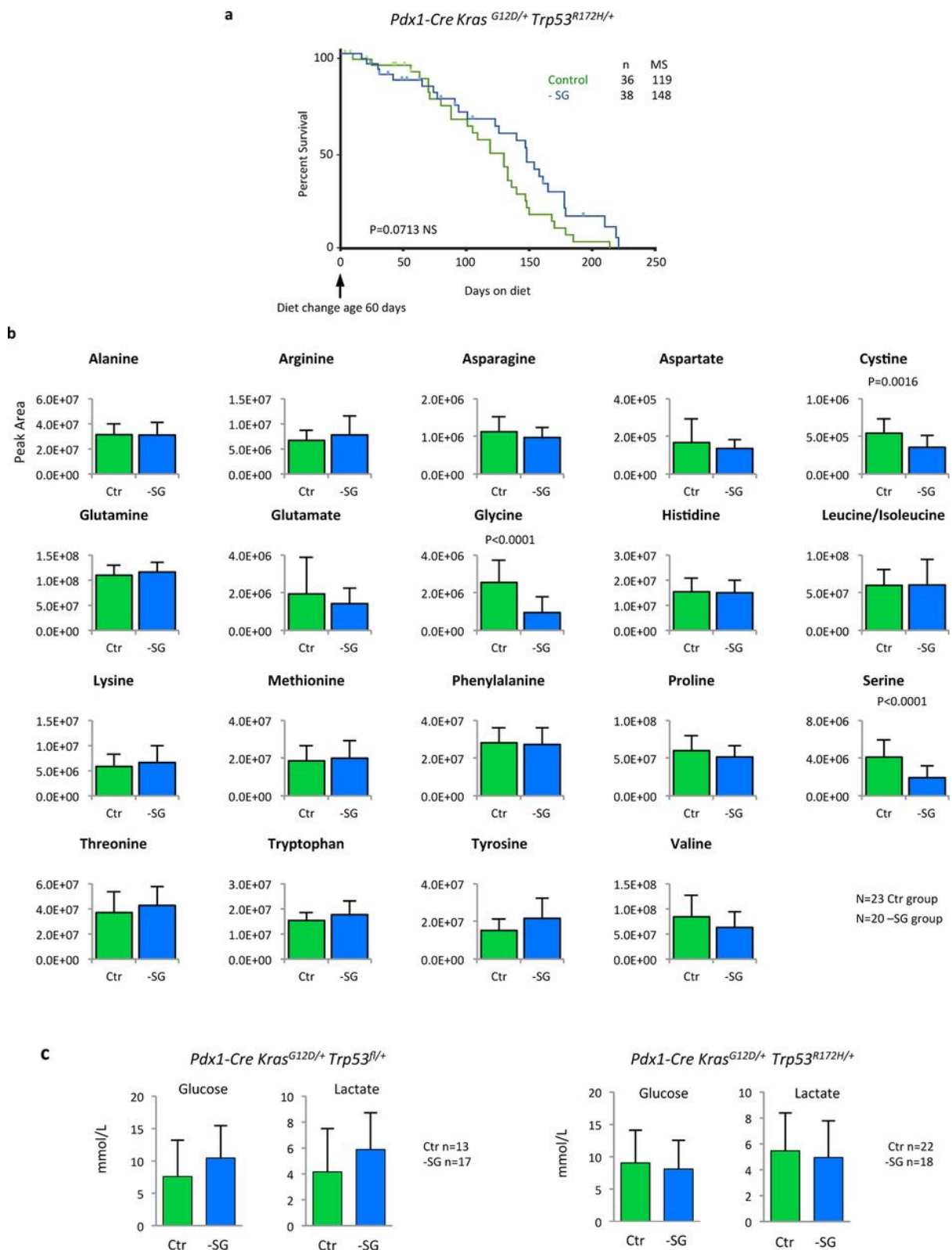
a, *Pdx1-cre;Kras^(G12D/+);Trp53^(R172H/+)* mice received control or SG-free (−SG) diet at 60 days of age until clinical end point. PDAC-related survival was calculated from change of diet. *P* value calculated by Mantel–Cox test. *n*, number of mice; MS, median survival in days. See Source Data. **b**, Serum isolated from terminal bleeds of *Pdx1-cre;Kras^(G12D/+);Trp53^(R172H/+)* mice was analysed by LC–MS. Relative

quantity of metabolites are shown (*y* axis = peak area). Error bars are s.d. *P* values were calculated for each amino acid by *t*-test (unpaired, two-tailed), *P* values <0.05 are 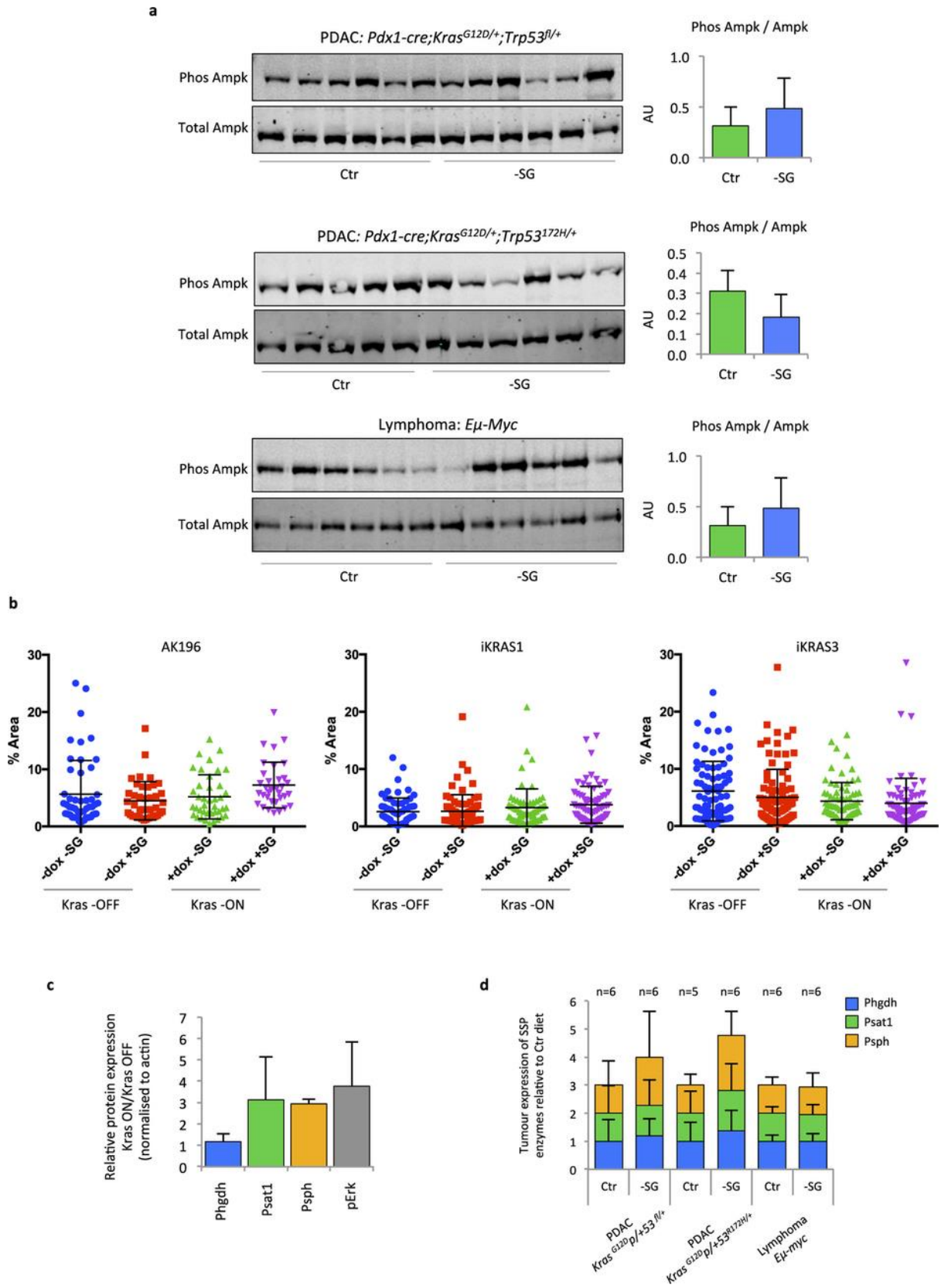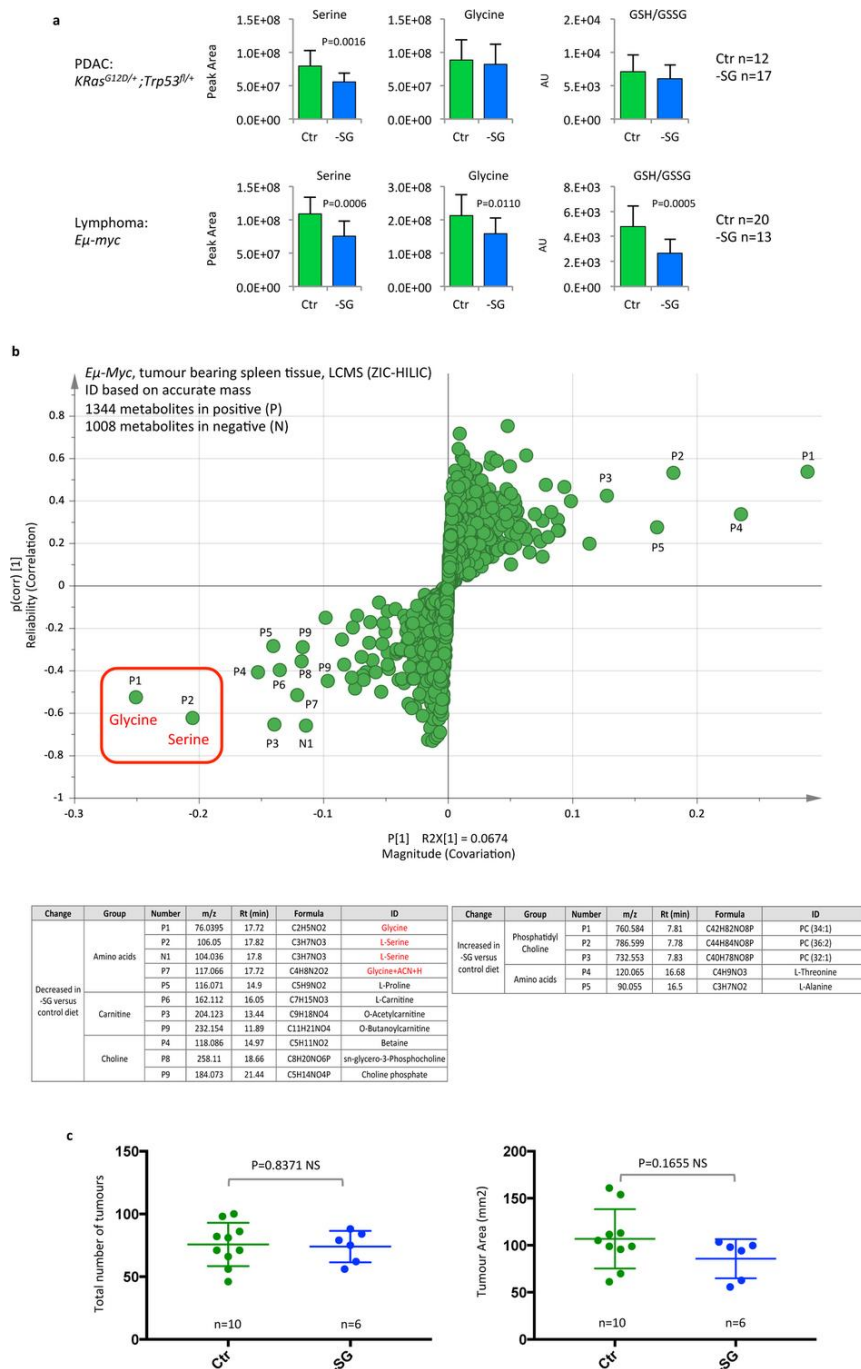shown. **c**, Serum samples from PDAC mice were analysed for glucose and lactate levels using a YSI 2950 Biochemistry Analyser.

Extended Data Figure 9: Effect of SG-starvation on AMPK phosphorylation, macropinocytosis and SSP protein expression.

a, Tumour-bearing spleens from *Eμ-Myc* mice and PDAC tissue were analysed by western blot for Ampk and phospho-Ampk levels, bands were quantified by LiCor infrared detection. For gel source data, see Supplementary Fig. 1. Data are averages, error bars are s.d. **b**, Macropinocytosis in iKras cells was assessed using TMR-labelled dextran uptake assay. Cells were initially grown with or without doxycycline for 48 h then seeded with or without doxycycline and with or without SG for 40 h (final 16 h without FBS), then given TMR dextran/FBS in matched medium for 30 min. Bars and lines show average and s.d. **c**, Relative changes Kras-ON/Kras-OFF (measured by LiCor infrared quantification) in expression of SSP and phospho-Erk1 protein averaged across iKras1, iKras3 and AK196 cells; the quantified bands are those shown in the western blot of Fig. 3d. Error bars are s.d. **d**, Protein lysates of tumour-bearing spleens from *Eμ-Myc* mice and PDAC tissue were analysed for SSP enzyme expression by western blot quantified using a Li-Cor scanner. Relative expression (versus control diet) of SSP enzymes is shown, bars are s.d. Each tissue sample was taken from a different mouse, numbers of mice/tumours are shown above the bars.

Extended Data Figure 10: Effect of SG-free diet on tumour metabolite levels and tumour burden in GEMMs.

Change	Group	Number	m/z	Rt (min)	Formula	ID
Decreased in -SG versus control diet	Amino acids	P1	76.0395	17.72	C2H5NO2	Glycine
		P2	106.05	17.82	C3H7NO3	L-Serine
		N1	104.036	17.8	C3H7NO3	L-Serine
		P7	117.066	17.72	C4H8N2O2	Glycine+ACN+H
		P5	116.071	14.9	C5H9NO2	L-Proline
	Carnitine	P6	162.112	16.05	C7H15NO3	L-Carnitine
		P3	204.123	13.44	C9H18NO4	O-Acetylcarnitine
		P9	232.154	11.89	C11H21NO4	O-Butanoylcarnitine
	Choline	P4	118.086	14.97	C5H11NO2	Betaine
		P8	258.11	18.66	C8H20NO6P	sn-glycero-3-Phosphocholine
		P9	184.073	21.44	C5H14NO4P	Choline phosphate

Change	Group	Number	m/z	Rt (min)	Formula	ID
Increased in -SG versus control diet	Phosphatidyl Choline	P1	760.584	7.81	C42H82NO8P	PC (34:1)
		P2	786.599	7.78	C44H84NO8P	PC (36:2)
		P3	732.553	7.83	C40H78NO8P	PC (32:1)
	Amino acids	P4	120.065	16.68	C4H9NO3	L-Threonine
		P5	90.055	16.5	C3H7NO2	L-Alanine

a, PDAC from *Pdx1-cre;Kras$^{G12D/+}$;Trp53$^{fl/+}$* mice and tumour-bearing spleens from *Eµ-Myc* mice were analysed by LC–MS for serine, glycine, GSH (reduced glutathione) and GSSG (oxidized glutathione). *P* values calculated by *t*-test, unpaired, two-tailed. Error bars are s.d. **b**, S-plot of unbiased metabolomic analysis (OPLS-DA, orthogonal partial least squares discriminant analysis) of *Eµ-Myc* tumour-bearing spleens (Ctr, *n* = 20; –SG, *n* = 13). The detected metabolites showing the greatest decrease due to diet are serine and glycine. Decreased levels of carnitine-related and choline-related metabolites were also observed. Increased levels of phosphatidylcholine (PC) metabolites and alanine and threonine were also seen (as in Extended Data Fig. 2b). SG starvation is known to influence glycolysis and oxidative phosphorylation (potentially explaining changes in

carnitine and alanine levels), and one-carbon metabolism (potentially explaining changes in choline-related metabolites). **c**, *Vil1-creER;Apc$^{fl/+}$;Kras$^{G12D/+}$* mice were placed on SG-free or control diet at 6–8 weeks of age, then induced with tamoxifen after two weeks and survived until clinical end point (intestinal-tumour-related survival). Post-mortem count of intestinal tumour number and tumour measurement was performed on intestine tissue. Error bars are s.d. *P* values were calculated by *t*-test (unpaired, two-tailed). See Source Data.